Title: Phase equilibrium engineering of glycerol acetates fractionation with pressurized COnull

Authors: Mariana Fortunatti Montoya, Francisco A. Sánchez, Pablo E. Hegel, Selva Pereda

PII: S0896-8446(17)30030-X
DOI: http://dx.doi.org/doi:10.1016/j.supflu.2017.02.026
Reference: SUPFLU 3906

To appear in: *J. of Supercritical Fluids*

Received date: 17-1-2017
Revised date: 26-2-2017
Accepted date: 27-2-2017

Please cite this article as: Mariana Fortunatti Montoya, Francisco A.Sánchez, Pablo E.Hegel, Selva Pereda, Phase equilibrium engineering of glycerol acetates fractionation with pressurized COx2082;, The Journal of Supercritical Fluidshttp://dx.doi.org/10.1016/j.supflu.2017.02.026

Phase equilibrium engineering of glycerol acetates fractionation with pressurized CO_2

Mariana Fortunatti Montoya,[1] Francisco A. Sánchez,[1] Pablo E. Hegel,[1] Selva Pereda[1,2]*

[1]Planta Piloto de Ingeniería Química (PLAPIQUI), Universidad Nacional del Sur (UNS) - CONICET, Camino La Carrindanga Km7, 8000B Bahía Blanca, Argentina

[2]Thermodynamics Research Unit, School of Engineering, University of KwaZulu-Natal, Howard College Campus, King George V Avenue, Durban 4041, South Africa

**e*-mail: spereda@plapiqui.edu.ar

Phase equilibrium engineering of glycerol acetates fractionation with pressurized CO_2

Mariana Fortunatti Montoya[1], Francisco A. Sánchez[1], Pablo E. Hegel[1], Selva Pereda[1,2]*

[1]Planta Piloto de Ingeniería Química (PLAPIQUI), Universidad Nacional del Sur (UNS) - CONICET, Camino La Carrindanga Km7, 8000B Bahía Blanca, Argentina

[2]Thermodynamics Research Unit, School of Engineering, University of KwaZulu-Natal, Howard College Campus, King George V Avenue, Durban 4041, South Africa

**e*-mail: spereda@plapiqui.edu.ar

Graphical Abstract

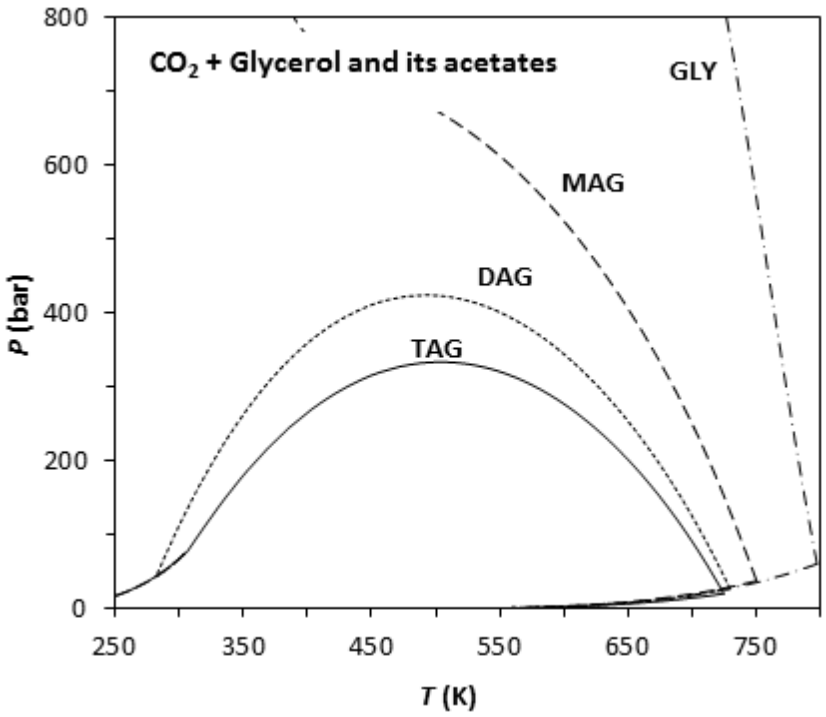

<InlineImage1>

Phase equilibrium engineering of glycerol acetates fractionation with pressurized CO_2

Mariana Fortunatti Montoya[1], Francisco A. Sánchez[1], Pablo E. Hegel[1], Selva Pereda[1,2]*

[1]Planta Piloto de Ingeniería Química (PLAPIQUI), Universidad Nacional del Sur (UNS) - CONICET, Camino La Carrindanga Km7, 8000B Bahía Blanca, Argentina

[2]Thermodynamics Research Unit, School of Engineering, University of KwaZulu-Natal, Howard College Campus, King George V Avenue, Durban 4041, South Africa

**e*-mail: spereda@plapiqui.edu.ar

Highlights

- Technology for glycerol valorization roadmap
- Purification of glycerol acetates with $scCO_2$
- Highly non-ideal systems are modeled with the GCA-EoS.
- Phase equilibrium engineering of fractionation units

Abstract

Glycerol acetates are considered important chemicals as part of the glycerol valorization roadmap. In this work, we evaluate their fractionation using CO_2 as extracting agent, based on a predictive thermodynamic model, since there is an important lack of experimental equilibrium information. We show that GCA-EOS predicts experimental data available for glycerol and tri-acetylglycerol, while achieves the phase behaviors of mono- and di-acetylglycerols by group contribution. The extension of the GCA-EOS was done by means of correlating phase equilibrium data of low molecular weight alcohols and esters. The predictive model is an essential tool to assess properly the supercritical fractionation of glycerol acetates. In this regard, we show here the effect of temperature, pressure and solvent-to-feed ratio for the design of a feasible phase scenario. Phase equilibrium engineering allows uncoupling the effect of variables, which is key for the design of future experimental studies on glycerol acetates fractionation using supercritical CO_2.

Keywords: glycerol acetate; phase equilibrium engineering; group-contribution; GCA-EOS

1. Introduction

The advent of biodiesel as a fuel additive for combustion engines leaded to a high production of glycerol, by-product of the transesterification reaction. Therefore, the beginning of the biodiesel peak caused a market saturation of glycerol and the fall of its price trigger the development of new valorization routes [1,2]. Some examples are glycerol reformation for hydrogen production [3,4] or etherification with isobutylene [2]. Another remarkable case is glycerol cyclization to produce epichlorydin, patented by Dow [5] and SOLVAY [6], a valuable epoxide due to its versatility as a precursor in the synthesis of many organic compounds. In addition, Lean and Luque [7] listed several other possible chemical paths to transform glycerol into valuable products (see Figure 1).

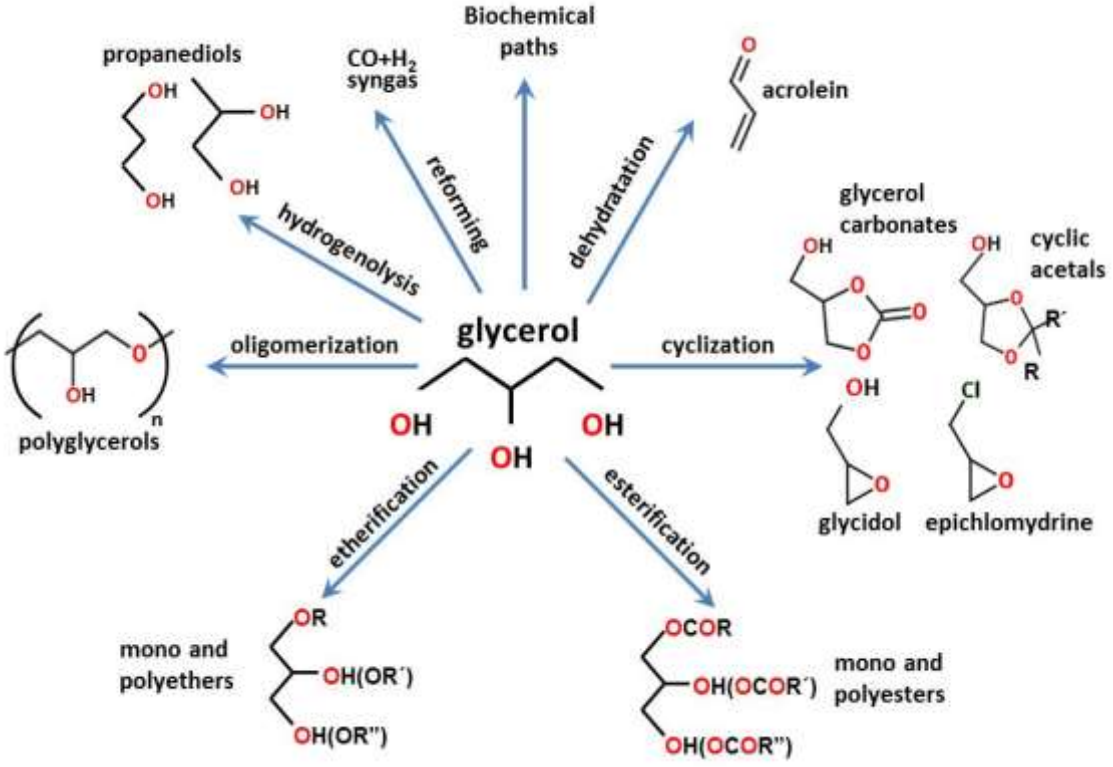

Figure 1. Roadmap of selected glycerol valorization reactions [7]

The route towards glycerol acetates (mono- and polyesters in Figure 1) also has high industrial importance. For example, triacetyglycerol (TAG) and diacetyglycerol (DAG) are currently under study as additives to improve fuel viscosity and cold properties; furthermore, TAG is a diesel antiknock additive [2]. Moreover, TAG has been considered a generally recognized as safe (GRAS) human food ingredient by the Food and Drug Administration (FDA) [8]. It is an attractive food additive as carrier of flavors and fragrances, commonly used in butter, candies and other food stuffs as well as in animal feed [9,10]. On the other hand, MAG and DAG are building blocks of polyesters and cryogenic fluids [11].

The mixture of glycerol acetates is difficult to fractionate by simply distillation because the components show low relative volatility and their elevated boiling points require a high operation temperature, which can cause thermal degradation at the detriment of the product quality. Thus, fractionation methods normally use organic solvents, which are less accepted by the consumers and have strict regulations for food related applications. Interestingly, Rastegari and Ghaziaskar [11] carried out the esterification reaction without catalyst using supercritical CO_2 ($scCO_2$) as a reaction media. They achieved 53% conversion and selectivity towards MAG of 92%. In a follow up work [12], they also reported the fractionation of a mixture of glycerol acetates using $scCO_2$ as solvent.

Up to our knowledge, there has not been any comprehensive study of the phase behavior of CO_2 + glycerol acetates, except for TAG. In this regard, Florusse et al. [13] and Hegel et al. [14] showed that CO_2 and TAG are completely miscible near the critical temperature of CO_2. On the other hand, the binary mixture of glycerol + CO_2 portrays a Type III phase behavior according to van Konynenburg and Scott[15] classification of binary systems, showing low mutual solubility [16,17]. Although there are not previous studies about MAG and DAG phase behavior with CO_2, the studies of Rezayat and Ghaziaskar [11] allows inferring that the two compounds show limited mutual solubility with CO_2. Given that MAG and DAG molecules are a functional group combination between glycerol (triol) and TAG (triester), it is expected that the mutual solubility of MAG and DAG with CO_2 will be in between that shown by TAG and glycerol with CO_2.

The rational design of a supercritical unit, either a reactor or a fractionator, requires a thermodynamic model in order to assess the feasible operating regions and minimum amount of required solvent. The lack of data for DAG and MAG points out the need of predictive models, precluding those equations of state based on a molecular approach. In contrast, group contribution methods are able to interpolate the behavior that MAG and DAG will show in between glycerol and TAG. Previous works have shown the robustness of the Group Contribution with Association Equation of State (GCA-EOS) [18] to correlate and predict complex multiphase equilibria in the context of supercritical fluid extraction [19–23]. In this work, we first extended the GCA-EOS, giving special emphasis to low molecular weight di-esters and di-alcohols, to predict phase behavior of glycerol acetates. Later on, based on the model predictions, we carried out the phase equilibrium engineering of glycerol acetates fractionation with pressurized CO_2.

2. Thermodynamic modeling

The compounds comprising the mixture under study, glycerol and its acetates, are a combination of either alcohol or ester groups. Figure 2 shows their group assembly. In the following sections we show the extension of GCA-EOS for the phase behavior prediction of the four components with CO_2.

It is important to lighten that the group contribution approach allows parameterizing both groups using equilibrium data available of other compounds containing these two groups. On the other hand, MAG and DAG represent two possible molecules because of positional isomers, as we show in Figure 2. Normally, we take advantage of the molecular free-volume contribution of GCA-EOS to distinguish isomers [24], by means of fitting their critical diameter to a vapor pressure data point. Since no experimental information is available for MAG and DAG isomers, we cannot differentiate them precisely. According to molecular simulations, 1-MAG and 1,3-DAG are the more abundant species of the two possible alternatives [25,26]; therefore, we simulate the mixture setting up these two compounds and leaving out 2-MAG and 1,2-DAG.

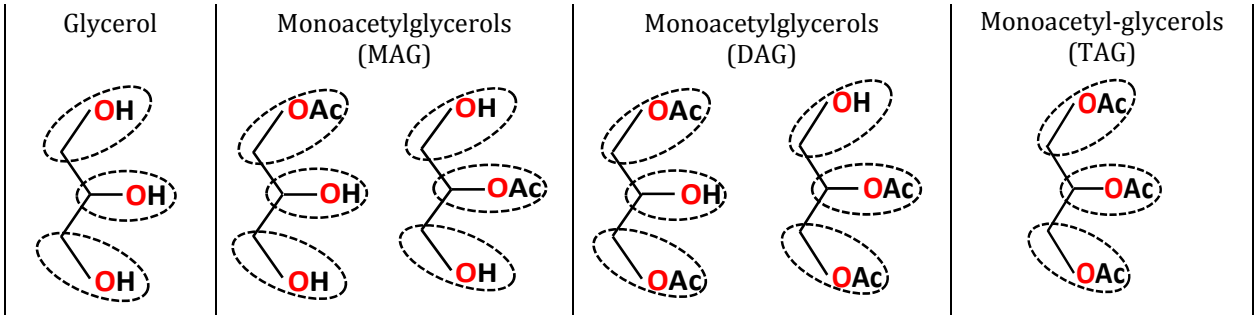

Figure 2. Group assembly of glycerol and its acetates. Characteristics groups: primary and secondary alcohol (CH_2OH and CHOH, respectively) and primary and secondary AcO (CH_2OOCH_3 and $CHOOCH_3$, respectively).

The calculation of equilibrium properties requires robust algorithms, able to perform multiphase-multicomponent calculations efficiently. In this work, all binary phase diagrams were calculated using GPEC [27,28], which allows performing several types of binary phase diagrams, together with the evaluation of critical lines. On the other hand, multicomponent flash calculation and supercritical fluid extraction processes were calculated using the algorithms developed by Michelsen [29,30] and Kehat and Ghitis [31].

2.1. The GCA-EOS

There are three contributions to the residual Helmholtz energy (A^R) in the GCA-EOS model [18]: free volume (A^{fv}), attractive (A^{att}) and association (A^{assoc}):

$$A^R = A^{fv} + A^{att} + A^{assoc} \quad (1)$$

The *free volume* contribution is the extended Carnahan-Starling [32] equation for mixtures of hard spheres developed by Mansoori and Leland [33], which is characterized by one pure-compound parameter: the critical diameter (d_c). The *attractive* contribution to the residual Helmholtz energy, A^{att}, accounts for dispersive forces between functional groups. It is a van der Waals expression combined with a density-dependent, local-composition mixing rule based on a group contribution version of the NRTL model [34]. This term is characterized by the number of surface segments of each group (q), and the surface energy (g), which is temperature dependent. Furthermore, each binary group interaction is characterized by one interaction parameter (k), which may be temperature dependent, and two binary damping factors (α). Finally, the *association* term, A^{assoc}, is a group contribution version of the SAFT equation developed by Chapman et al. [35]. This term is characterized by two parameters: the energy (ε) and volume (κ) of association. Naturally, the latter will only be present in the case of components showing specific association interaction (hydrogen-bonding or solvation). A more detailed explanation of the model can be found elsewhere [36].

2.2. Parameterization procedure

The parameterization was performed through the optimization of the following objective function:

$$\text{O.F.} = \sum_{i=1}^{NSat} e_{\text{sat},i}^2 + \sum_{i=1}^{NEq} e_{\text{eq},i}^2 \tag{2}$$

where *NSat* and *NEq* are the number of pure vapor pressure and binary VLE data, respectively. Furthermore, $e_{\text{sat,i}}$ and $e_{\text{eq,i}}$ are the error between experimental and calculated data, as follows:

$$e_{\text{sat},i}^2 = \left(\frac{P_{\text{exp},i}^{\text{sat}} - P_{\text{calc},i}^{\text{sat}}}{P_{\text{exp},i}^{\text{sat}}} \right)^2 \tag{3}$$

$$e_{\text{sat},i}^2 = \left(\frac{P_{\text{exp},i}^{\text{sat}} - P_{\text{calc},i}^{\text{sat}}}{P_{\text{exp},i}^{\text{sat}}} \right)^2 + \left(\frac{y_{\text{exp},i} - y_{\text{calc},i}}{y_{\text{exp},i}} \right)^2 \tag{4}$$

P is the pressure and *y* the molar fraction in the vapor phase. We minimized the objective function (Eq. (2)) using the Levenberg–Marquardt algorithm coded in Fortran77.

As shown above, in order to assemble the compounds under study, we need primary and secondary alcohol groups and ester groups with different degree of substitution. It is worth noting that the primary and secondary alcohol groups, likewise the ester groups, share characteristics parameters in this work. For instance, the parameters of the residual contribution, both the surface energy parameters and the binary interaction, are the same. Regarding association parameters (either self- or cross-association) primary and secondary alcohol groups share the energy of association but not the volume, approach proposed by Gregg et al. [37] based on the fact that secondary alcohol groups are less available to associate due to steric hindrance.

In this work, we extend the model primary alcohol group to describe the secondary alcohol group and propose a new parameterization for the ester groups. The reader can find which specific data was used to correlate each parameter in the appendix (Tables A1 to A6). In the following sections we discuss each correlation and challenge the GCA-EoS predictive capacity.

3. Results and discussion

In the following sections we discuss the extension of the model to secondary alcohols, the reparameterization of alkyl esters and the model predictive capacity against phase behavior data available for compounds comprising multiple ester and alcohol groups. The Appendix reports all the parameters required to model the system under study, those already available in the GCA-EOS table of parameters and the new parameters fitted in this work.

3.1. Modeling alcohols containing multiple hydroxyl groups

Given the assumption that the primary and secondary alcohol group only differ in the self or cross-association volume, modeling pure polyols and its mixture with CO_2 only required fitting two new parameters. We first fitted the self-association volume of the secondary alcohol group to 2-propanol vapor pressure data [38]. Table 1 shows GCA-EoS deviations in this correlation, as well as in the prediction of the vapor pressure and critical point of other secondary alcohols and polyols.

Furthermore, Figure 3 compares the model accuracy to predict vapor pressure of primary alcohols reported by Soria et al. [39] and secondary alcohols predictions from this work (Figure 3.a and 3.b, respectively). As can be seen, the accuracy of the GCA-EOS for predicting primary and secondary alcohols is equivalent, showing the robustness of maintaining all the parameters of the primary alcohol group, but the volume of association for the secondary alcohol group. Based on the primary and secondary alcohol groups, we assembled and predicted phase behavior of polyols. For instance, Figure 3.b also depicts the model predictions of the diols vapor pressure (full symbols). For these compounds the predictions are less accurate; nonetheless, the result is good enough for a preliminary study of the fractionation process.

Table 1. GCA-EOS average relative deviation in vapor pressure and source of experimental data.

Compound	ΔT_r	AARD(P)%	ARD(T_c)%	ARD(P_c)%	Ref.
Correlation					
2-propanol	0.53-0.97	1.5	0.6	1.3	[38]
Prediction					
2-butanol	0.53-0.97	4.3	2.1	6.0	[38]
2-pentanol	0.54-0.97	4.2	2.1	5.7	[38]
3-pentanol	0.53-0.97	6.5	3.2	14	[38]
2-hexanol	0.54-0.97	3.3	2.0	5.9	[38]
MEG	0.50-0.64	4.0	3.5	6.9	[40,41]
1,2-propanediol	0.52-0.73	9.6	3.8	10	[42,43]
1,2-butanediol	0.55-0.74	9.3	4.0	16	[44]
1,3-butanediol	0.41-0.99	13	2.4	3.1	[45,46]
1,4-butanediol	0.26-0.99	6.8	2.8	2.7	[47]

Regarding binary systems with CO_2, González Prieto et al. [48,49] have recently extended the GCA-EOS to mixtures of CO_2 with the homologous family of alkanes and 1-alkanols. Since CO_2 is an acid gas, they modeled it as an electron acceptor, with two electropositive sites, able to solvate with alcohols. Likewise for the self-association, we set for the association between CO_2 and the secondary alcohol group the same energy parameter but we fitted a new reduced volume of association to binary data of CO_2 + 2-propanol at 293 K. Figure 4 depicts the model accuracy to predict binary mixtures of CO_2 with secondary alcohols. Particularly, Figure 4.a shows phase behavior of CO_2 + 2-propanol binary mixture. The dashed line indicates the correlated isotherm, while continuous lines depict the model extrapolations to higher temperatures. Moreover, Figure 4.b shows GCA-EOS predictions of CO_2 + 2-butanol, another secondary alcohol. As can be seen, the model follows experimental data quantitatively well except at the lower temperatures in the CO_2 diluted region, where predictions are merely qualitative.

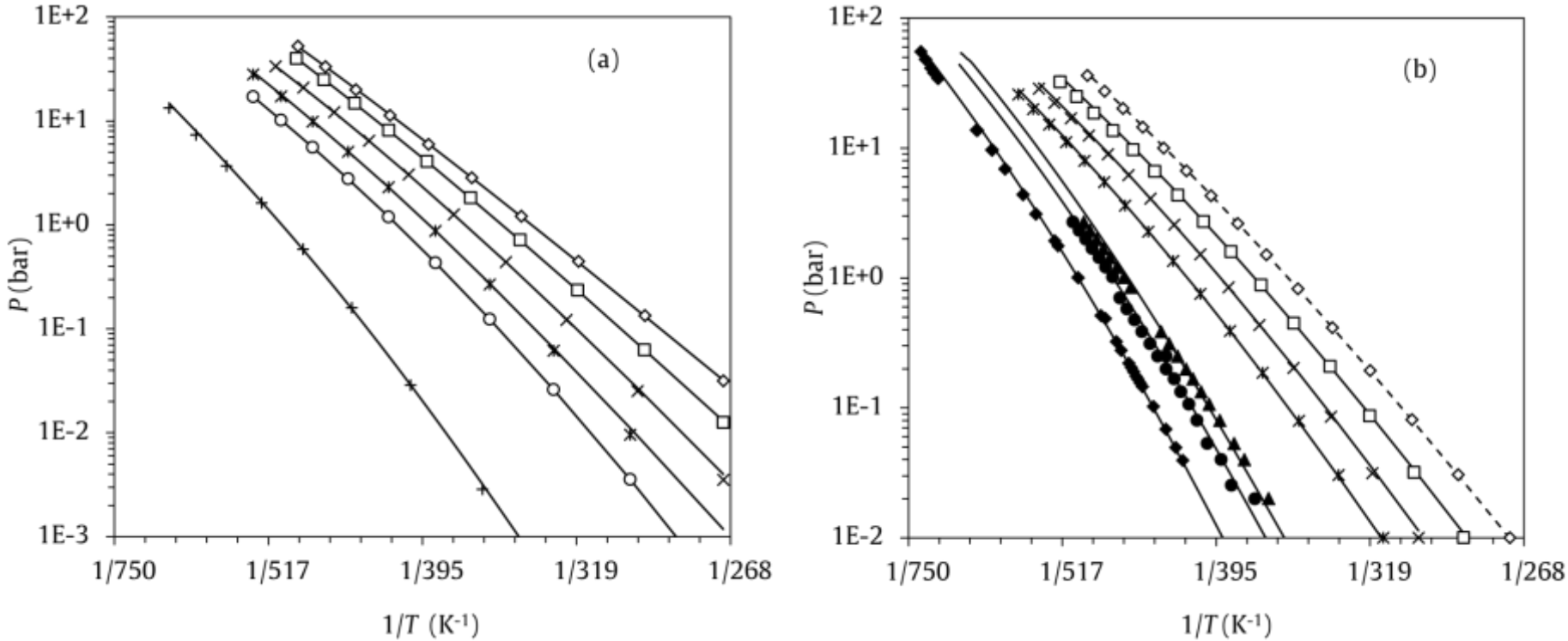

Figure 3. Vapor pressure of alcohols: **(a)** Primary alcohols [38]. (◇) methanol, (□) ethanol, (×) 1-propanol, and (∗) 1-butanol, (○) 1-pentanol, and (+) 1-decanol. Solid lines, GCA-EOS calculations using the parameters provided by of Soria et al. [39]. **(b)** Secondary alcohols [38] and alkanediols [42–46]: (◇) 2-propanol, (□) 2-butanol, (×) 2-pentanol, (∗) 2-hexanol, (▲) 1,2-propanediol, (●) 1,2-butanediol, (◆) 1,4-butanediol [47]. Dashed and solid lines: GCA-EOS correlation and prediction, respectively. Full symbols: alkanediols vapor pressure

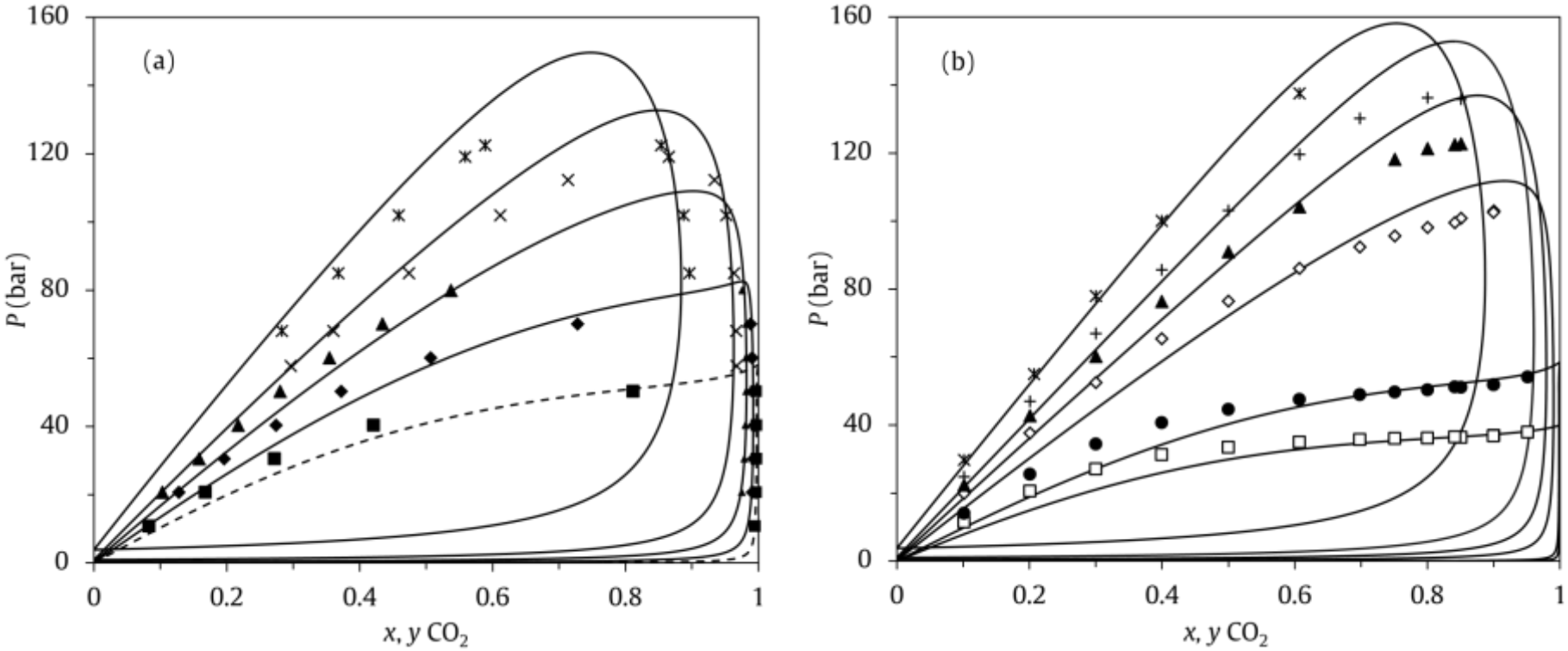

Figure 4. Vapor liquid equilibria of CO_2 + secondary alcohols binary system: **(a)** 2-propanol [50] at (■)293 K, (◆) 313 K, (△) 333 K, (×) 355, and (○) 394 K. (AARD(P) =9.0% and AARD(y_{CO2})=0.41%). **(b)** 2-butanol [51] at (□) 278 K, (●) 293 K, (◇)333 K, (▲)353 K, (+) 373 K, and (∗)414 K. AARD(P) = 8.6%, AARD(y_{CO2}) = data not available). Dashed and solid lines: model correlation and prediction, respectively.

Figure 5 shows the GCA-EoS prediction of the phase behavior of two butanediol isomers. Although the data is a bit scattered, there is a clear difference in the binary phase behavior of both isomers in mixtures with CO_2. Based on the primary alcohol group parameterization of Gonzalez Prieto et al. [39,49] and its extension to the new secondary alcohol group, the model predicts accurately the CO_2 solubility in the liquid phase for both, 1,2-butanediol and 1,3-butanediol. Moreover, the GCA-EoS also predicts a higher content of 1,2-butanediol in the CO_2 phase, in agreement with the experimental data. It is worth noting that these are full predictions, i.e. none of the binary data was used to correlate the model parameters.

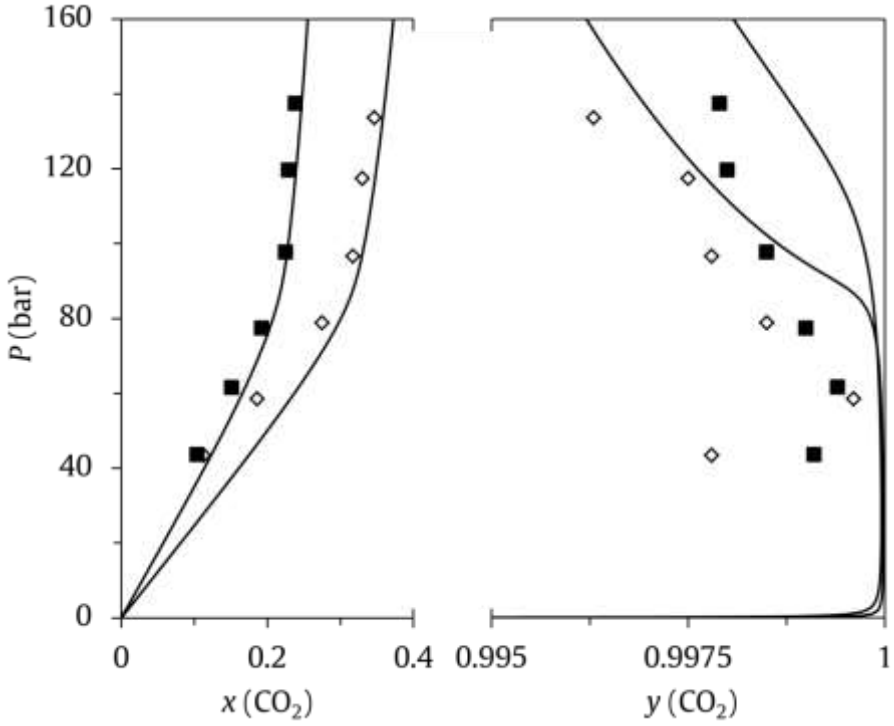

Figure 5. Vapor-liquid equilibria of CO_2 + butanediol at 313 K [52]. Symbols: (◇) 1,2-butanediol (AARD(x_{CO2}) = 18%, AARD(y_{CO2})= 0.1%) and (■) 1,3-butanediol (AARD(x_{CO2}) = 5.8%, AARD(y_{CO2})= 0.1%). Lines: GCA-EOS predictions.

3.2. Modeling of esters containing multiple acetate groups

Previous works extended the GCA-EOS to monoesters in the context of process development for biodiesel production [53] and fish oil [19] fractionation. Both applications involve fatty esters with alkyl chain length between 16 and 20 carbons. If the same set of parameters is used for low molecular weight monoacetates, the model qualitatively predicts their vapor pressure, i.e about 10% deviation for ethyl and propyl acetate. Even though this is not an important offset, it is unacceptable in this work, since the poor description of the ester group amplifies when dealing with compounds comprising multiple ester groups. Therefore, we carried out a new parameterization of this group, defined here as CH_xCOOCH_y, where *x* and *y* varies between 1 and 3 (see Table A1 in the Appendix). In contrast with the previous definition, we capped with alkyl groups the oxygenated carbon from both sides, enhancing the electroneutrality of the group that was previously only capped from one side [54]. In this work, we appointed the same characteristic parameters of pure group for all the esters groups, which only differ in the number of surface segments, *q*, as discussed by Bondi [55]. Similarly,

all these groups share the binary interaction parameters of the attractive and association contributions.

The Appendix details the specific experimental data used to correlate each of the parameters required to describe the new ester group (see Tables A1 to A3). We correlated the pure group parameters with methyl acetate and dimethyl succinate vapor pressure data. Table 2 compares GCA-EoS predictions of the vapor pressure and the critical points of several low molecular weight esters, with the new parameterization and that using the prior set of parameters. The calculations show that we significantly improved the accuracy of the model to predict the vapor pressure of low molecular weight monoesters, a 2.6% deviation in average. Figure 6 shows the vapor pressure prediction of several mono- and di-esters. On the other hand, we fitted the interaction parameters between esters and paraffinic group to binary VLE data of ester + alkanes. Figures 7.a depicts GCA-EOS accuracy to correlate *n*-pentane + butyl acetate, while Figure 7.b shows the model prediction of other two acetates with *n*-hexane (ethyl and *n*-butyl acetate). Finally, we correlated the binary interaction parameters between ester and CO_2 groups using high-pressure VLE data of CO_2 + ethyl acetate and TAG, simultaneously. Figure 8 shows GCA-EOS correlation and prediction of CO_2 + ethyl/propyl acetate mixtures. Unfortunately, up to our knowledge, there is no phase equilibrium data available for CO_2 + diester mixtures, which would be useful to challenge the model predictive capacity. In the following section we will discuss the model capacity to correlate and predict the triester TAG, which is one of the components comprised in the mixture under study here.

Table 2. GCA-EoS prediction of vapor pressure and critical point of esters. Comparison between this work parameters and prior set[54]. Source of vapor pressure and critical properties: DIPPR [38], except for dimethyl [56,57] and diethyl succinate [58]

Compound	ΔT_r	AARD(p^v)%		ARD(T_c)%		ARD(P_c)%	
		This work	Prior Set [54]	This work	Prior Set [54]	This work	Prior Set [54]
Correlation							
methyl acetate	0.47-0.95	1.7	8.5	0.07	3.4	1.0	29.1
dimethyl succinate	0.53-0.95	3.0	5.2	0.05	5.1	1.2	39.6
Prediction							
ethyl acetate	0.49-0.95	2.4	11	0.15	3.2	4.6	27
isopropyl acetate	0.49-0.95	1.0	12	0.20	3.2	1.9	29
n-propyl acetate	0.50-0.95	2.6	8.3	0.01	3.1	3.4	25
isobutyl acetate	0.50-0.95	2.2	10	0.35	3.2	3.7	27
n-butyl acetate	0.50-0.95	2.0	6.5	0.14	3.2	0.78	25
ethyl propanoate	0.50-0.95	3.0	6.1	0.34	2.5	8.0	16
propyl propanoate	0.49-0.92	0.66	5.2	3.0	2.0	1.3	18
ethyl butyrate	0.50-0.95	7.1	1.7	0.04	4.3	8.8	35
methyl dodecanoate	0.56-0.96	3.3	3.9	0.03	2.1	0.65	3.6
diethyl succinate	0.55-0.96	2.6	3.1	1.9	4.6	13	27

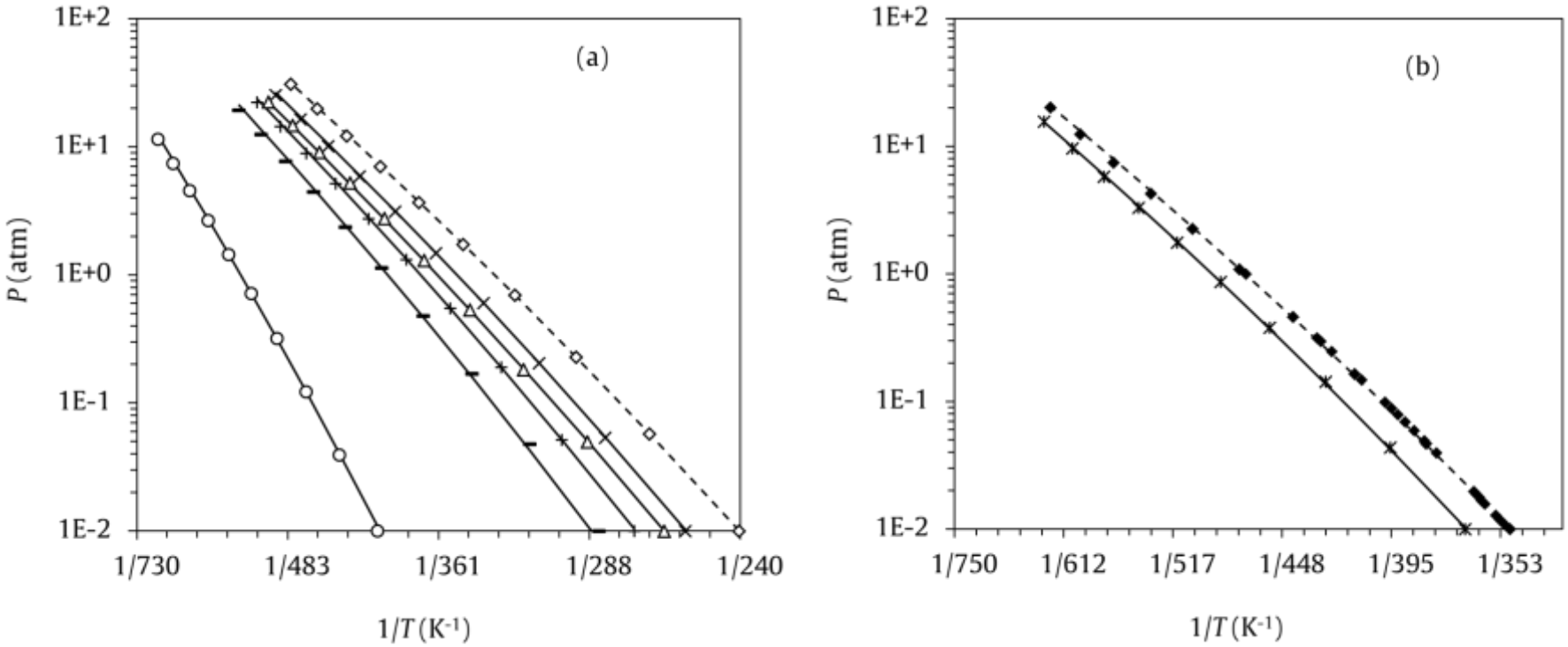

Figure 6. Vapor pressure of esters [38]. **(a)** Monoesters: (◇) methyl acetate, (×) ethyl acetate, (△) isopropyl acetate, (+) ethyl propionate, (–) ethyl butanoate, and (○) methyl dodecanoate. **(b)** Diesters: (◆) dimethyl and (∗) diethyl succinate. Dashed and solid lines: GCA-EOS correlation and prediction, respectively.

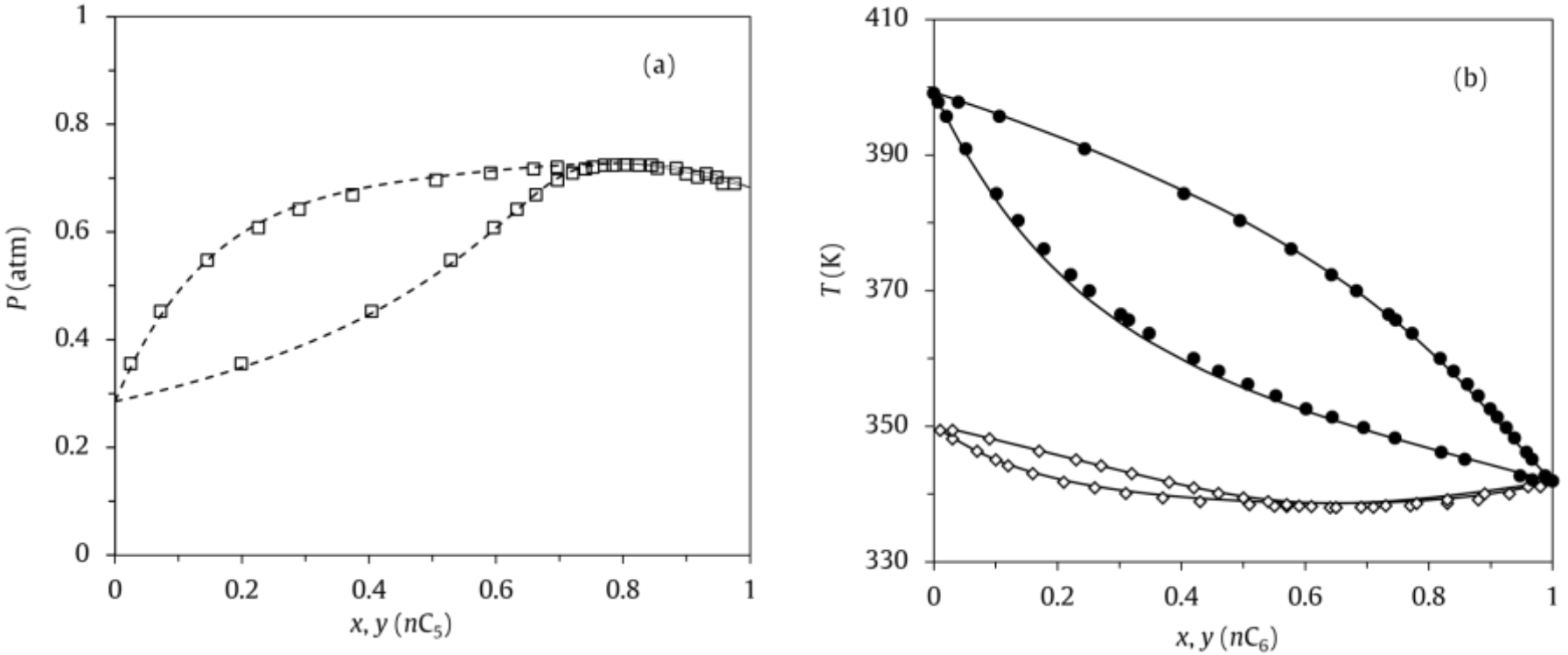

Figure 7. VLE of monoesters + alkanes binary mixtures: **(a)** *n*-pentane + methyl acetate at 298 K [59] (AARD(*P*) = 1.2%, AARD(y_{CO2}) = 0.7%). **(b)** VLE of *n*-hexane + (◇) ethyl acetate (AARD(*T*) = 0.12%, AARD(y_{CO2} = 1.2%)) and (●) *n*-butyl acetate (AARD(*T*) = 0.18%, AARD(y_{CO2} = 3.4%)) [60,61] at 1 atm. Dashed and solid lines: GCA-EOS correlation and prediction, respectively.

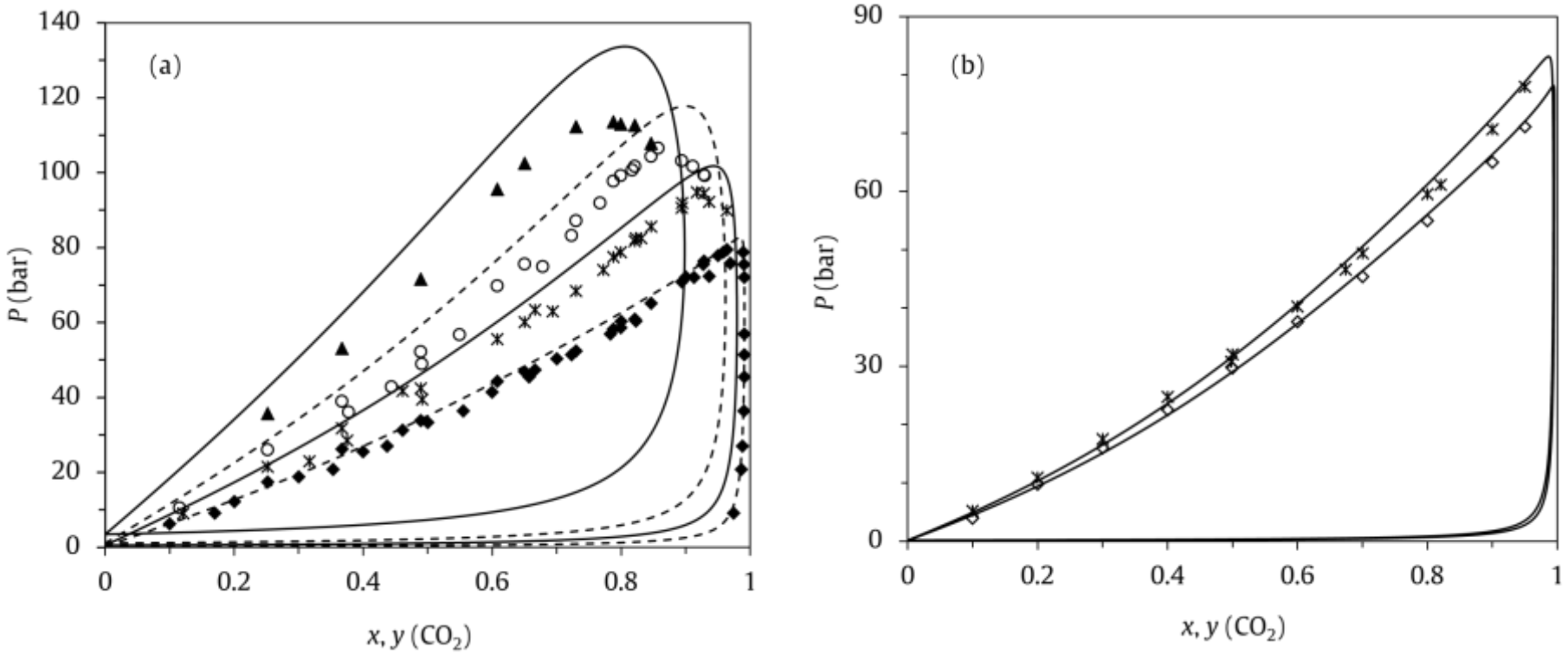

Figure 8. Vapor-liquid equilibria of CO_2 + monoesters: **(a)** ethyl acetate [62–66] at (◆) 313 K, (∗) 333 K, (○) 353 K, (■) 373 K, and (▲) 393 K (AARD(P) = 7.8% and AARD(y_{CO2}) = 0.03%), **(b)** isopropyl acetate [67] at (◇) 308 K and (+) 313 K (AARD(P) = 3.5%), A. Dashed and solid lines: GCA-EOS correlation and prediction, respectively.

3.3. Modeling glycerol and its acetates mixtures

Since the mixture under study includes both, alcohols and acetate groups, the interaction between them is also needed. We applied the same approach as described previously: we first correlated the ester/primary alcohol interaction and then we transferred the binary interaction parameters to the secondary alcohol group, except for the cross-association volume which was fitted to VLE data of isopropyl acetate + 2-propanol. Figure 9 shows the correlation and prediction of primary and secondary alcohols with esters. The GCA-EOS models well the VLE of alcohol+ester mixtures using a proper cross-association strength and the same binary interaction parameter for primary and secondary alcohol groups in the residual contribution.

Interesting data to challenge the model extension to molecules comprising more than one alcohol or ester group is that of ethylene glycol (MEG) and its acetates: ethylene glycol monoacetate (MAEG) and ethylene glycol diacetate (DAEG). It is worth to highlight the similarity of the group assembly of these components and that of glycerol and its acetates. Figure 10 compares experimental and predicted pure component vapor pressure and binary VLE of MEG and its acetates. GCA-EoS shows an average absolute relative deviation of about 4% for the three components. Furthermore, Figure 10.b shows that these three components have low relative volatility and their binary mixtures are close to depicting azeotropic behavior. In both cases, the GCA-EOS follows the experimental data with an acceptable accuracy. From this result we are confident that GCA-EOS is able to predict phase behavior of glycerol and its acetates, at least qualitatively.

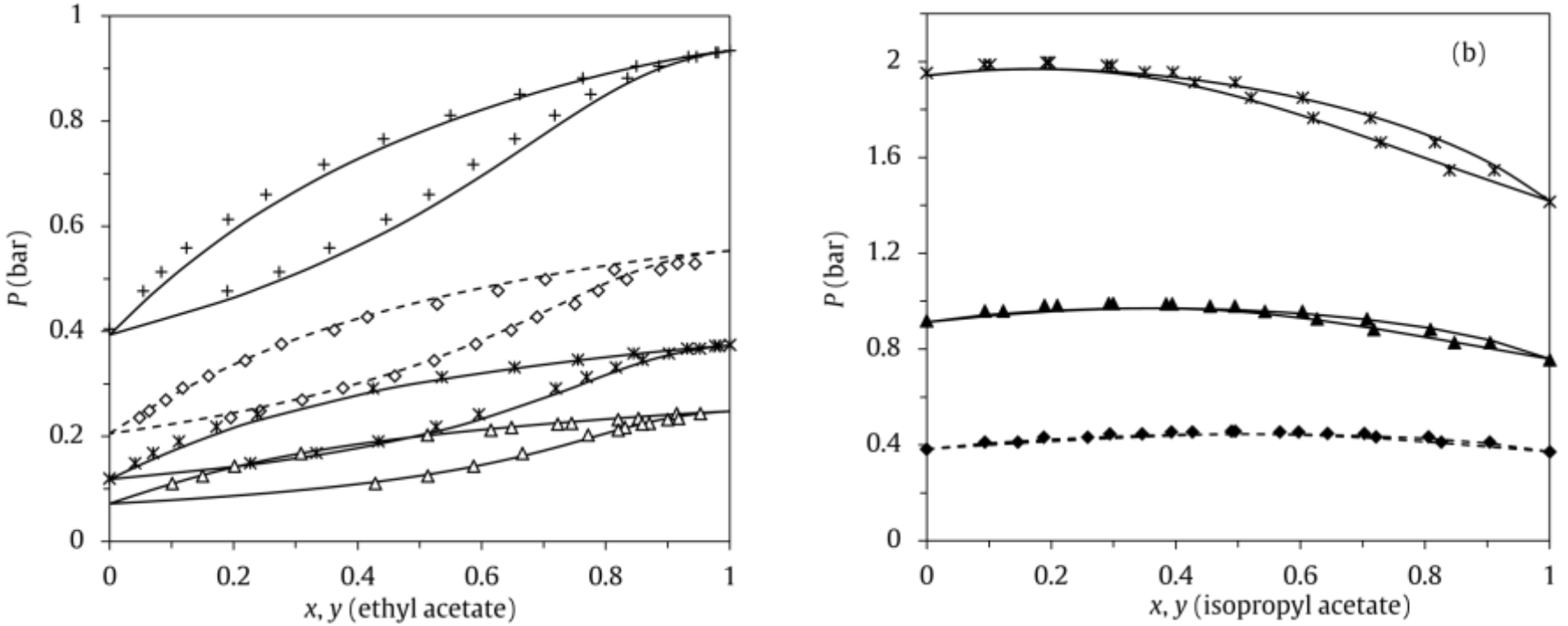

Figure 9. Vapor liquid equilibria of alcohol + acetates binary systems: **(a)** ethyl acetate + 1-propanol [68,69] at (△) 313 K, (∗) 323 K, (◇) 333 K, and (+) 343 K (AARD(P) = 1.6%, AARD(y_{CO2}) = 1.0%). **(b)** isopropyl acetate + 2-propanol [70] at (◆) 333 K, (▲) 353 K, and (∗) 373 K (AARD(P) = 1.8%, AARD(y_{CO2}) = 1.6%). Dashed and solid lines: GCA-EOS correlation and prediction, respectively.

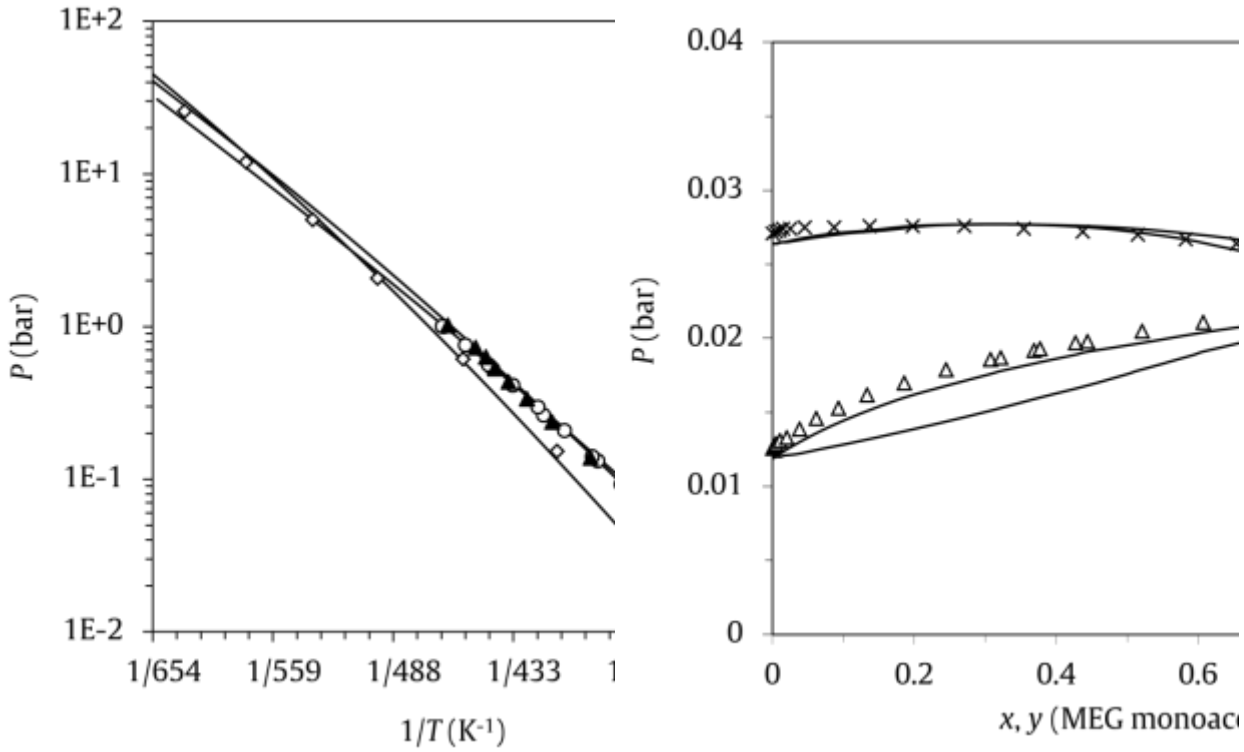

Figure 10. Vapor liquid equilibria of ethylene glycol (MEG) and its mono and diacetate (MAEG and DAEG, respectively). **(a)** Vapor pressure of (◇) MEG [40,41] (AARD(P)=4.0%), (▲) MAEG [71] (AARD(P)=3.7%) and (○) DAEG [72] (AARD(P)=4.1%). **(b)** (△) MEG + MAEG (AARD(*P*) = 4.3%) and (×) MAEG + DAEG (AARD(*P*) = 1.6%) [71] at 363 K. Lines: GCA-EOS predictions.

Like in previous cases, we first evaluated the model capacity to predict the pure component vapor pressures, key property for a correct prediction of binary and multicomponent mixtures. Figure 11.a compares vapor pressure data of glycerol and TAG with GCA-EOS predictions. The average absolute relative deviations are about 20%, which is a rather accurate result, taking into account that the vapor pressures of both components depict values as low as 10^{-5} bars, under the evaluated temperature range (see Figure 11.a). Furthermore, Figure 11.b shows the GCA-EOS predictions of the unavailable vapor pressures of MAG and DAG. It is worth noting that, as expected, the vapor pressures of the components to be fractionated are very similar, hindering the possibility of applying simple distillation to separate the mixture of acetates.

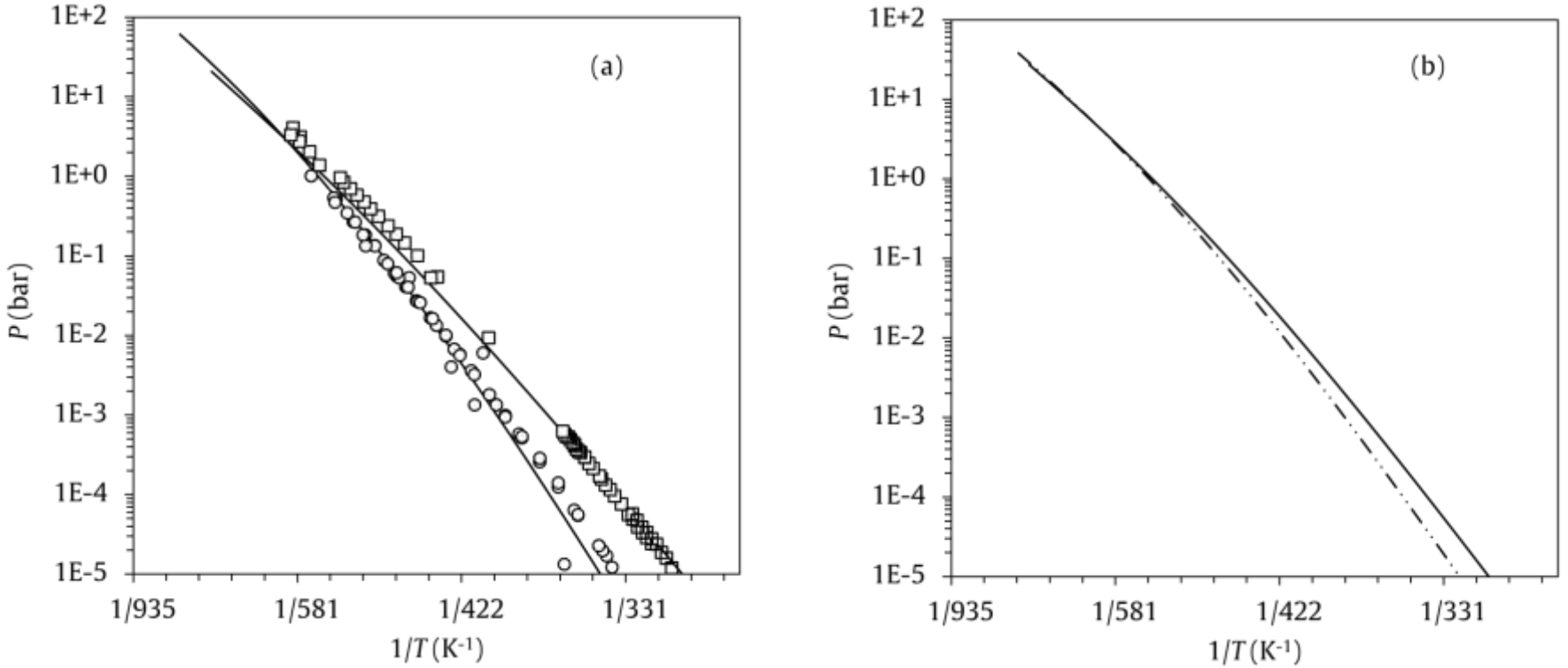

Figure 11. Vapor pressure of glycerol and its acetates. **(a)** GCA-EOS (solid line) and experimental data of glycerol (○)[38] (AARD(P)=19%) and TAG (□)[72–77] (AARD(P)=21%). **(b)** GCA-EOS prediction of MAG (dashed dotted line) and DAG (solid line) vapor pressure.

Regarding phase behavior of binary systems with CO_2, high pressure data for glycerol and TAG are available in the literature. Figure 12 depicts the model performance to calculate both binaries. The result shown for glycerol is a full prediction (Figure12.a), since we did not include this compound in any step of the parameterization of the alcohol groups. On the other hand, to improve the model accuracy, we had to include part of the experimental data of CO_2 + TAG mixture in the parametrization of the binary interaction of the ester group. Figure 12.b shows that the GCA-EOS extrapolates well the temperature dependence of this binary system phase behavior.

Finally, Figure 13 compares the GCA-EOS predictions of MAG and DAG phase behavior with that of glycerol and TAG at 333 K. Figure 13.a shows that the model is in accordance with the available experimental data, i.e. the complete miscibility between TAG and CO_2 above 140 bars and the partial miscibility of the latter with glycerol. The mutual solubility of MAG and DAG lay between glycerol and TAG. Particularly, the binary CO_2 + DAG becomes completely miscible above 200 bars, while CO_2 + MAG keeps immiscible up to high pressure, like the binary with glycerol. Figure 13.b depicts the *PT* diagram of each binary system, where the reader can see the overall behavior of the four components. This figure shows that the increase of the esterification grade, from glycerol to TAG, causes a change from Type III (glycerol and MAG) to V (DAG and TAG) phase behavior, according to van Konynenburg and Scott [15] classification of binary systems.

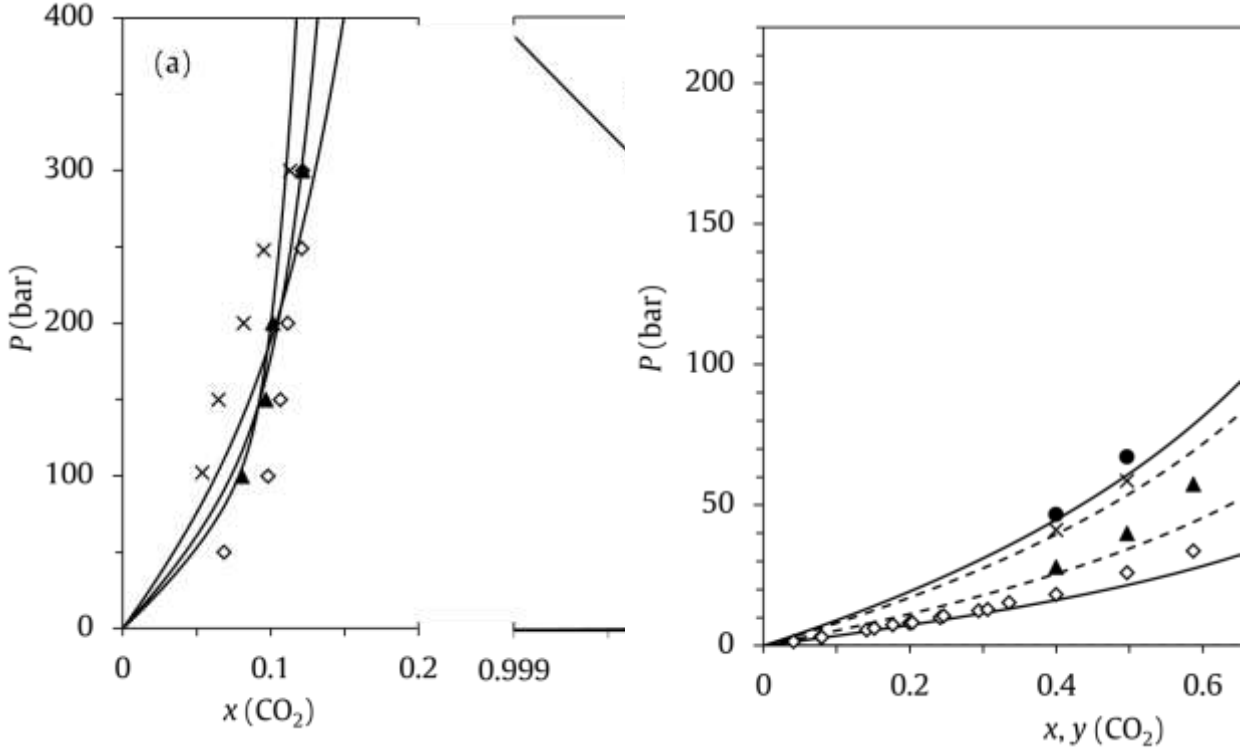

Figure 12. Binary high pressure vapor liquid equilibria **(a)** CO_2 + glycerol [17] at 333K (◇), 353K (▲), and 393K (×) (AARD(x_{CO2} = 15%), AARD(y_{CO2}) = 0.5%). **(b)** CO_2 + TAG [13,14,78] at 298 K (◇), 323 K (▲), 353 K (×) and 363 K (●) (AARD(P) = 6.6%). Dashed and solid lines: GCA-EOS correlation and prediction, respectively.

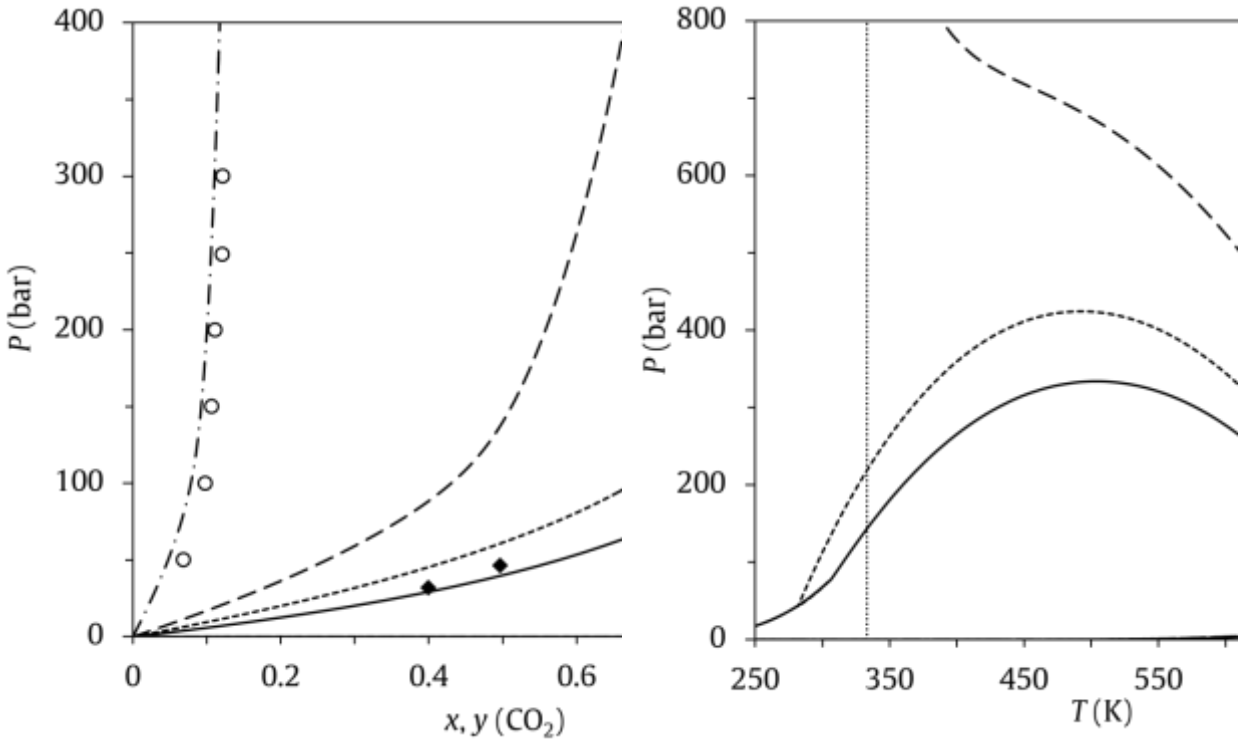

Figure 13. GCA-EOS prediction of phase behavior of CO_2 with MAG and DAG and comparison with that of glycerol and TAG. Lines: TAG (solid), DAG (dots), MAG (dashes) and glycerol (dashes and dots). **(a)** *Pxy* diagram at 333 K. Experimental data: TAG (◆) [13,14] and glycerol (○) [17]. **(b)** *PT* diagram of CO_2 + glycerol and its acetates binary systems.

3.4. Phase Equilibrium Engineering

Glycerol acetates are synthesized via esterification of glycerol with acetic acid, which is a reversible reaction. It is possible to achieve almost full esterification and produce high purity TAG using a high excess of acetic acid. However, if the aim is obtaining MAG or DAG, the chemical equilibrium hinders the possibility of achieving either of them with high purity. Therefore, the design of purification processes to produce MAG and DAG is of importance. In this work, we analyze the fractionation of two different mixtures. The first one is the product of the conventional synthesis [12]; therefore, its composition is similar to commercial samples provided by chemical companies. On the other hand, Rastegari et al. [11] proposed recently to carry out the reaction in supercritical CO_2. They enhanced the selectivity towards MAG operating at 393 K, 80 bar, and a molar ratio of acetic acid to glycerol of 2. Table 3 reports the composition of both mixtures.

Table 3. Composition of the studied mixtures (weight basis).

Mixture	% MAG	% DAG	%TAG	Source
A ($scCO_2$ medium)	67	30	3	[11]
B (conventional route)	19	50	31	[12]

Phase equilibrium engineering [79] of the supercritical fractionation process put the thermodynamic model to work. In that sense we analyze below feasible scenarios for process conceptual design, i.e. we discuss the effect of temperature, pressure and solvent-to-feed mass ratio (*S*/*F*) in a supercritical fractionator, based on GCA-EOS predictions. Since phase behavior of each glycerol derivative with CO_2 varies greatly, feasible phase scenario for the two mixtures under study will be different. For instance, we show in Figure 14 the phase envelope of the two mixtures with an arbitrary amount of solvent of 3.75 (CO_2 to feed mass ratio). As expected, Mixture A shows a larger heterogeneous region because MAG is less miscible with CO_2 than DAG and TAG. According to the model predictions, Mixture A shows the existence of two phases even above 600 bars at CO_2 near critical temperature. On the other hand, for the same amount of CO_2, the phase boundary of Mixture B is at much lower pressures and it is highly dependent on temperature. In conclusion, assuring heterogeneous conditions is more sensitive for mixture B than A due to its lower content of MAG. Figure 15 shows the effect of the amount of CO_2 on the feasible operating region of Mixture B. Particularly, Figure 15.a depicts the effect of *S*/*F* on the phase envelope, while Figure 15.b illustrates the maximum pressure to ensure heterogeneous phase operation at selected near critical temperatures. Although we emphasize that the quantitative accuracy of all these results have to be verified experimentally, we are confident on the GCA-EOS predictions regarding the sensitivity of the phase behavior. It is worth noting that the presence of a partially soluble substrate like TAG, which act as co-solvent for the other acetates, makes more complex the proper design of experimental work to assess the fractionation process. In that sense the statistical experimental design may lead to unfeasible operating conditions if phase equilibrium thermodynamics is not taken into account.

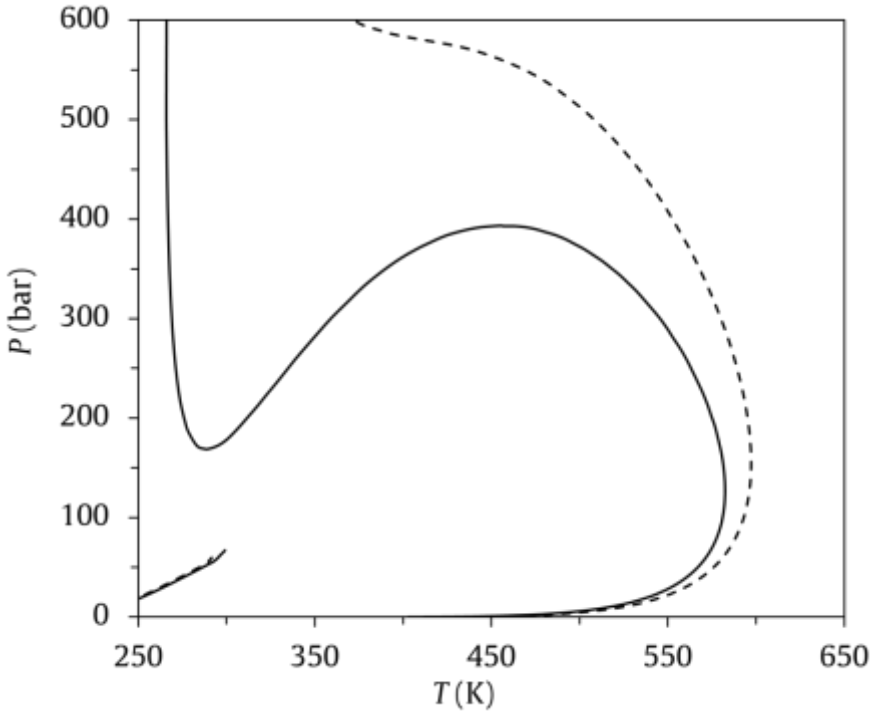

Figure 14. GCA-EOS prediction of phase envelope of the mixtures A (dashed) and B (continuous) for a S/F = 3.75.

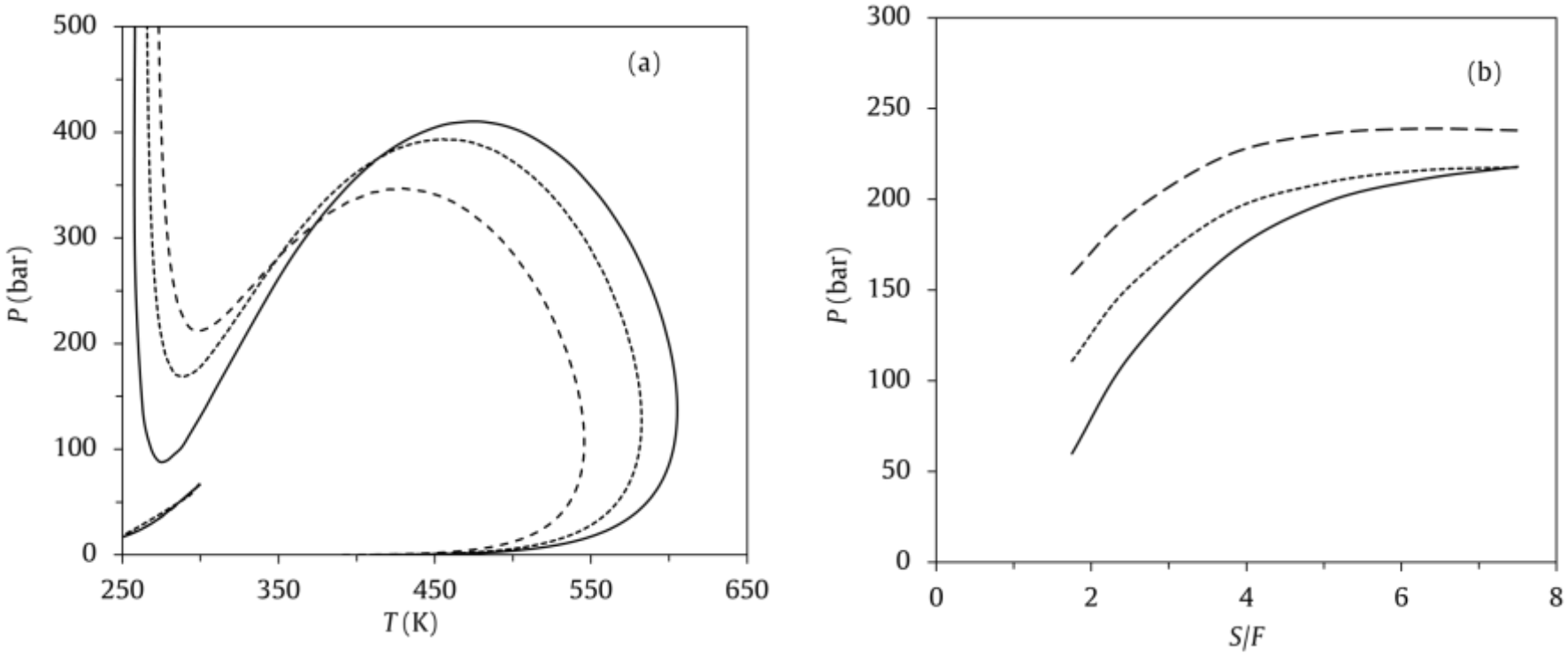

Figure 15. Effect of the amount of solvent on the feaseable operating region for Mixture B. **(a)** GCA-EOS prediction of phase envelopes for constant solvent to feed mass ratio. S/F = 2.5 (solid), 3.75 (dotted), and 7.5 (dashed). **(b)** Maximum pressure to ensure heterogenous conditions at selected near critical temperatures. Lines: 293 K (solid), 308 K (dotted) and 323 K (dashed).

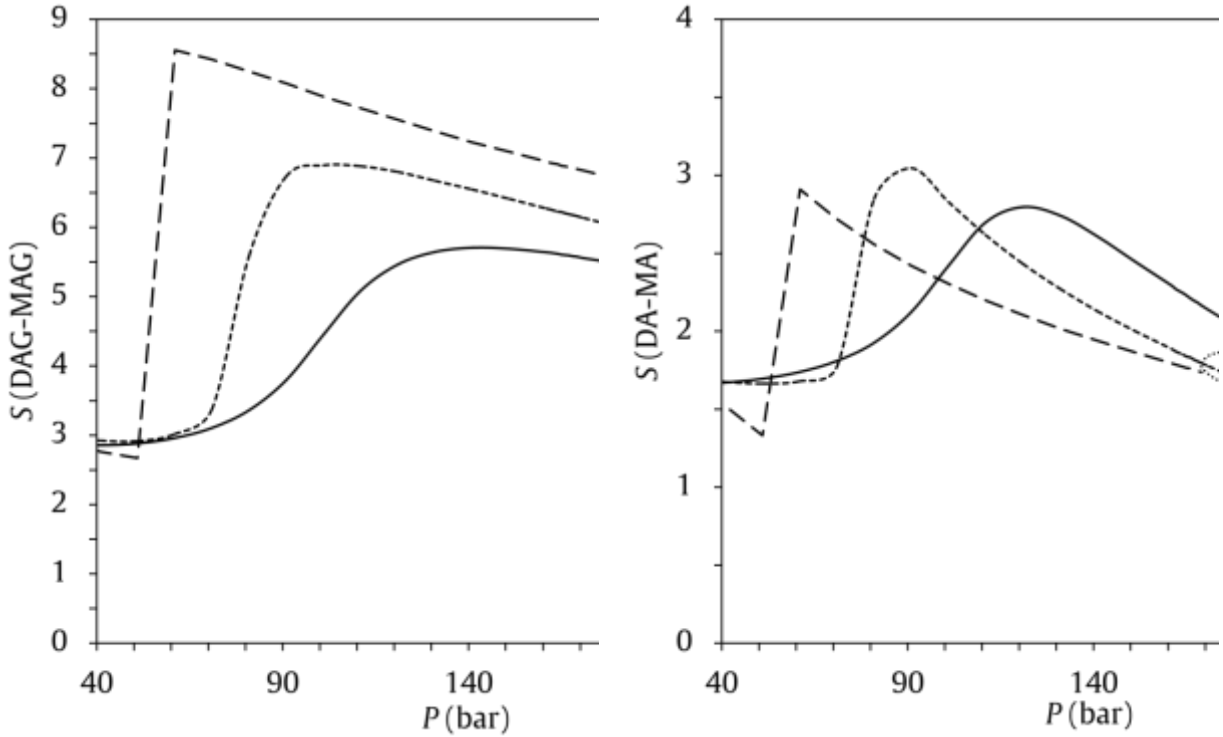

Figure 16. Selectivity of DAG to MAG against pressure for *S*/*F* = 3.75 and selected temperatures. **(a)** Mixture A. **(b)** Mixture B. Lines: 293 K (dashed), 308 K (dotted), and 323 K (solid).

Designing a fractionation process also requires knowledge of substrates selectivity, in order to set conditions that assure the efficient use of the solvent. Figure 16 shows the single stage selectivity of DAG with respect to MAG as a function of pressure, at different temperatures, for a fix amount of CO_2. For both mixtures, there is a maximum selectivity when increasing pressure, which occurs in the transition between the vapor-liquid-equilibrium (at low pressure) and the liquid-liquid like phase equilibrium. As can be seen, Mixture A shows much higher selectivity than Mixture B, as a consequence of the co-solvency among the different substrates. This lower selectivity is then evidenced in Figure 17, which shows the recovery of TAG, DAG, and MAG from Mixture B in a counter-current extraction process of 5 theoretical stages, at 308 K and *S*/*F* = 3.75. The simulation under this condition clearly shows the lack of an operating window to recover high purity MAG with a reasonable yield.

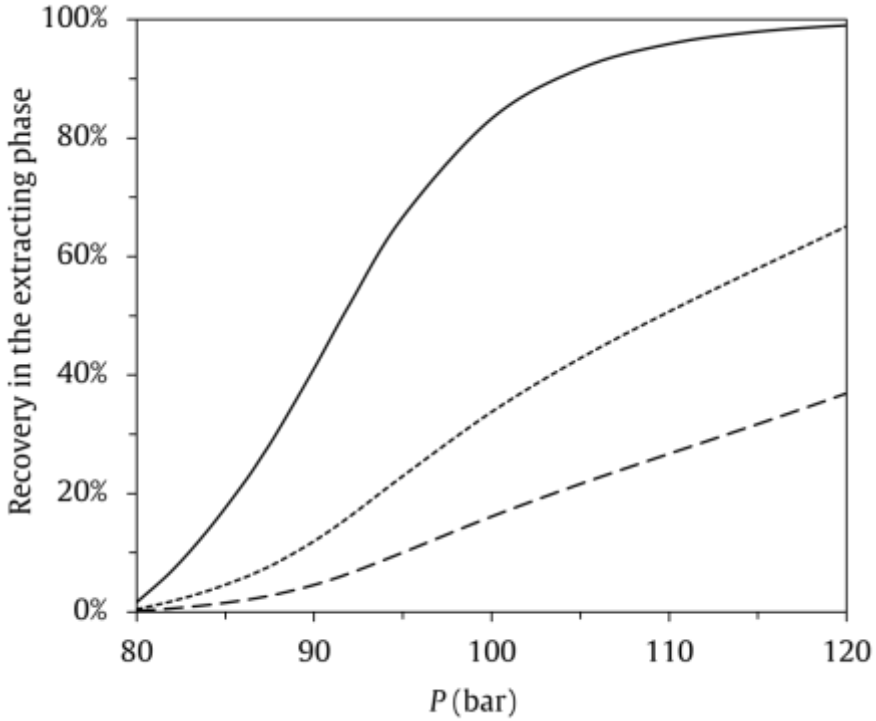

Figure 17. Counter-current fractionation of Mixture B in a 5 theoretical stages column at 308 K and *S*/*F* = 3.75. Recovery of TAG (solid), DAG (dotted) and MAG (dashed) in the extract phase.

To end up, we simulate the fractionation of both mixtures in a 5-theoretical stages column at 308 K and 95 bar, which corresponds to the maximum selectivity for Mixture B. Figure 18 reports MAG recovery and purity against the amount of solvent in the feed (*S*/*F*). According to the GCA-EOS predictions, in the case of mixture A, it is possible to recover high purity MAG with a high yield using supercritical CO_2. In contrast, Figure 18.b makes clear that this is not possible for Mixture B, unless a reflux is added.

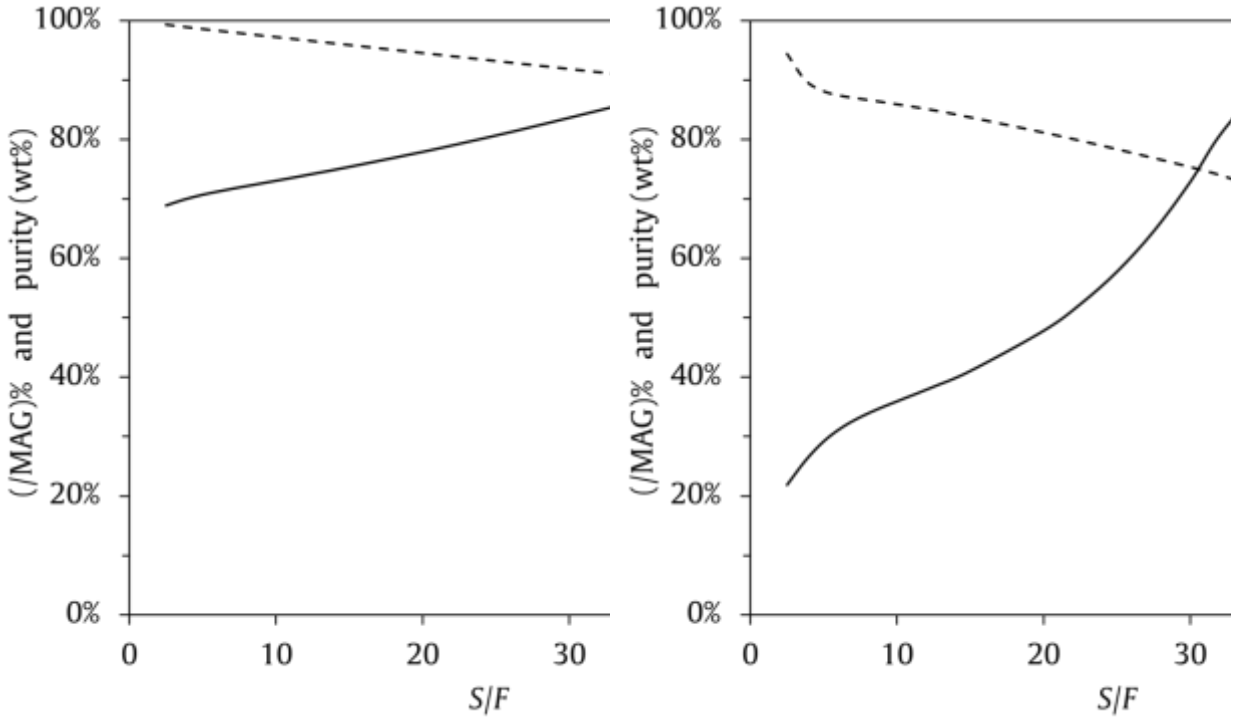

Figure 18. MAG recovery (dashed lines) and purity (continuous line) in the raffinate at 308 K, 95 bar and 5 theoretical stages. **(a)** Mixture A **(b)** Mixture B.

4. Conclusions

The production of glycerol acetates is an alternative route to valorize the current surplus of glycerol. This study reports the benefits of applying a group contribution model to predict phase behavior of mixtures containing glycerol acetates, for which there is a complete lack of key experimental data. We show that GCA-EOS is a robust model to predict phase behavior of CO_2 with either glycerol or TAG. According to the predictions of the binary mixtures, the $scCO_2$ is an attractive solvent to fractionate glycerol acetates. Nevertheless, multicomponent simulations show that the co-solvency between the substrates may lead to poor selectivities, depending upon the composition of the mixture to be fractionated. Furthermore, the simulations also make clear that a simple countercurrent extraction is not enough to produce high purity MAG with a reasonable yield, in the case of mixtures with high content of TAG.

The thermodynamic analysis shows that phase equilibrium behavior is strongly dependent on the mixture composition, a sensitivity that makes more complex the task of searching for the correct operating window. In this regard, the use of statistical design of experiments to assess the process, even though sometimes useful, may lead to unfeasible experiments and does not give a fair picture of a complex system like this. In contrast, Phase Equilibrium Engineering provides a rigorous approach to uncouple the effect of variables, useful to design experiments and analyze their results.

List of symbols

A	Helmholtz free energy
AARD(Z)%	Average absolute relative deviation in variable Z: $\frac{100}{N}\sum_i^N \left\|1-\frac{Z_{\text{calc}\,i}}{Z_{\text{exp}\,i}}\right\|$
ARD(Z)%	Absolute relative deviation in Z: $100\times\left\|1-\frac{Z_{\text{calc}}}{Z_{\text{exp}}}\right\|$
(/A)%	Percent recovery of compound A.
DAG	Diacetylglycerols
d_{ci}	Effective hard sphere diameter of component i evaluated at T_c
g_j	Group energy per surface segment of group j
K_i	Distribution coefficient of component i
LLE	Liquid-liquid equilibria
MAG	Monoacetylglycerols
MEG	Monoethylenglycol
N	Number of stages
NC	Number of components in the mixture
NG	Number of attractive groups in the mixture
NGA	Number of associating groups in the mixture
q_j	Number of surface segments of group j
R	Universal gas constant
$R_{\text{vdW},i}$	van der Waals reduce volume of compound i
r_j	Number of volume segments of group j
S (A-B)	Selectivity of A with respect to B: K_A/K_B

S/F	Solvent-to-feed ratio (mass basis)
T	Temperature
TAG	Triacetylglycerol
T_{ci}	Critical temperature of component *i*
VLE	Vapor-liquid equilibria
w_i	Mass composition of component *i*
x_i	Molar composition in liquid phase of component *i*
$\Delta Z\%$	AARD% in variable *Z*

Greek symbols

α_{ij}	Non-randomness parameter between groups *i* and *j*
$\varepsilon_{ki,lj}$	Energy of association between site *k* of group *i* and site *l* of group *j*
$\kappa_{ki,lj}$	Volume of association between site *k* of group *i* and site *l* of group *j*
ν_{ij}	Number of groups *j* in compound *i*
ν_{ij}^{*}	Number of associating groups *j* in compound *i*

Appendix

This appendix reports all the GCA-EOS parameters required to model the system under study. Tables A1 and A2 summarize those of the attractive contribution (pure group surface energy and binary interaction), while Table A3 lists parameters for the association interactions (association energy and volume). In each case we also include the source of the parameters taken from previous works. In contrast, for those parameters fitted in this work, we indicate the correlated experimental data in the table footnotes. On the other hand, Tables A4 to A6 reports properties of all the compounds evaluated in this work: molecular weight, group assembly, and the parameters for the repulsive contribution (critical diameter and critical temperature). Tables A4 and A5 summarizes data for alcohols and esters, respectively, while Table A6 for acylglycerides. Since pure component data for MAG and DAG is not available, we predict their critical temperature following the approach of González Prieto et al. [36]. Moreover, calculation of the molecular critical diameter usually requires at least one vapor pressure data point. However, Pereda et al. [80] and Espinosa et al. [54] proposed a correlation to calculate d_c parameter, based on the density and van der Waals volume, respectively, for low volatile compounds, whose vapor pressure is frequently unknown. Since there is no density or vapor pressure information for MAG and DAG, we apply the approach of Espinosa et al. [54] to calculate their critical diameter.

Table A1. Pure Group Parameters of the GCA-EOS.

Group	T^* (K)	q	g^* (atm cm^6/mol^2)	g'	g''	Reference
CH_3	600	0.848	316910	-0.9274	0	[81]
CH_2	600	0.540	356080	-0.8755	0	[81]
$CHCH_3$	600	1.076	303749	-0.8760	0	[82]
CO_2	304.2	1.261	531890	-0.5780	0	[81]
$CH_2OH/CHOH^a$	512.6	1.124/0.812	531330	-0.3201	-0.0168	[39]

CH_3COOCH_3	600	2.576	490000	-0.670	-0.180	this work[b]
CH_3COOCH_2		2.268				
CH_2COOCH_3		2.268				
CH_2COOCH_2		1.960				
CH_3COOCH		1.956				

[a] Secondary alcohol (CHOH) parameters are extrapolated from the values reported by Soria et al. [39], simply changing the number of surface segments, *q*.
[b] Fitted to methyl acetate and dimethyl succinate vapor pressure data [38].

Table A2. Binary energy interaction parameters used in this work.

Group		k_{ij}*	k_{ij}'	α_{ij}	α_{ji}	Reference
i	*j*					
CO_2	CH_3	0.9185	0.0469	-26	4	[48]
	$CH_2/CHCH_3$	0.9100	0.0469	-21	0	[48]
	$CH_2OH/CHOH$	0.9084	0.0800	-5	0	[49]
	CH_3COOCH_2/CH_3COOCH	0.9084	-0.080	-3	0	this work[1]
$CH_2OH/CHOH$	CH_3	0.8950	-0.0900	0	0	[39]
	CH_2	1.0200	0.0050	0	0	[39]
	$CHCH_3/CHCH_2$	0.9424	-0.1000	0	0	[81]
	CH_3COOCH_2/ CH_3COOCH	0.9850	0.0799	0	0	this work[2]
CH_3COOCH_2/ CH_3COOCH	CH_3/CH_2	0.9387	0.0225	0.6875	0.6875	this work[3]

[1] Fitted to CO_2 + ethyl acetate[62,83] and CO_2 + triacetin [14,84] VLE data.
[2] Fitted to ethyl acetate + 1-propanol [52] and isopropyl acetate + 2-propanol [70] VLE data.
[3] Fitted to methyl acetate + *n*-pentane [59] VLE data.

Table A3. Association contribution parameters used in this work.

Site *k*	Group *i*	Site *l*	Group *j*	$\varepsilon_{ki,lj}\,R^{-1}$ (K)	$\kappa_{ki,lj}$ (cm^3/mol)	Reference
(+)	CO_2	(–)	OH	1583	1.5214	[49]
		(–)	OH-2nd	1583	1.0	this work[a]
		(–)	RCOOR’	1000	4.0	this work[b]
(+)	OH	(–)	OH	2759	0.8709	[39]
		(–)	OH-2nd	2759	0.7823[c]	this work
		(–)	RCOOR’	2000	3.7035	this work[d]
(+)	OH-2nd	(–)	OH-2nd	2759	0.7028	this work[e]
		(–)	RCOOR’	2000	2.5	this work[f]

[a] Fitted to CO_2 + 2-propanol [50] and CO_2 + 2-butanol [51].
[b] Fitted to CO_2 + ethyl acetate and CO_2 + TAG [14,84] VLE data.
[c] Fu and Sandler [85] combination rule.
[d] Fitted to ELV of ethyl acetate + 1-propanol [52] VLE data.
[e] Fitted to 2-propanol [38] vapor pressure.
[f] Fitted to isopropyl acetate + 2-propanol [70] VLE data.

Table A4. Pure component properties: molecular weight, critical temperature, group assembly and GCA-EOS repulsive contribution parameters (d_c) of the alcohols studied in this work.

Compound	M (g/mol)	T_c (K)	d_c [a] (cm/mol$^{1/3}$)	GCA-EOS groups				Ref
				CH_3	CH_2	CH_2OH	CHOH	
2-propanol	60.1	508.2	4.032	2		1		[38]
2-butanol	74.1	536.2	4.446	2	1	1		[38]
2-pentanol	88.1	560.3	4.791	2	2	1		[38]
3-pentanol	88.1	559.6	4.826	2	2	1		[38]
2-hexanol	102.2	585.9	5.086	2	3	1		[38]
MEG	62.1	720.0	3.800			2		[38]
1,2-propanediol	76.1	676.4	4.156	1		1	1	[42,43]
1,2-butanediol	90.1	680.0	4.548	1	1	1	1	[44]
1,3-butanediol	90.1	692.0	4.443	1	1	1	1	[45,46]
1,4-butanediol	90.1	723.8	4.427		2		2	[47]
glycerol	92.1	850.0	4.312			1	2	[38]

[a] Calculated from the normal boiling point of the pure compound.

Table A5. Pure component properties: molecular weight, critical temperature([38],[56],[58]), group assembly and GCA-EOS repulsive contribution parameters (d_c) of the esters studied in this work

Compound	M (g/mol)	T_c (K)	d_c [a] (cm/mol$^{1/3}$)	GCA-EOS groups				
				CH_3	CH_2	$CHCH_3$	CH_3COOCH_x	CH_2COOCH_y
methyl acetate	74.1	506.6	4.309				1 (x=3)	
ethyl acetate	88.1	523.3	4.584	1			1 (x=2)	
isopropyl acetate	102.1	532.0	4.907	2			1 (x=1)	
n-propyl acetate	102.1	549.7	4.905	1	1		1 (x=2)	
isobutyl acetate	116.2	560.8	5.198	1		1	1 (x=2)	
n-butyl acetate	116.2	575.4	5.193	1	2		1 (x=2)	
ethyl propanoate	102.1	546.0	4.829	2				1 (y=2)
propyl propanoate	116.2	586.7	5.145	2	1			1 (y=2)
ethyl butyrate	116.2	571.0	5.142	2	1			1 (y=2)
methyl dodecanoate	214.4	712.0	6.807	1	9			1 (y=2)
dimethyl succinate	146.1	657.0	5.370				2 (x=2)	
DAEG	146.1	649.4[b]	5.412				2 (x=2)	
diethyl succinate	174.2	663.0	5.814	2				2 (y=2)
TAG	218.2	724.0[b]	6.380				2 (x=2)	1 (y=1)

[a] Calculated from the normal boiling point of the pure compound, except for methyl acetate, which is calculated from its critical point, likeall molecular groups[].
[b] Not available in open literature, value predicted by GCA-EOS.

Table A6. Pure component properties: molecular weight, critical temperature, group assembly and GCA-EOS repulsive contribution parameters (d_c) of the acylglicerides studied in this work.

Compound	M (g/mol)	T_c (K) [a]	d_c (cm/mol$^{1/3}$)	GCA-EOS groups		
				CH_2OH	CHOH	CH_3COOCH_2
MAEG	104.1	640.0	4.707[b]	1		1
MAG	134.1	748.6	5.109[c]	1	1	1
DAG	176.2	725.1	5.765[c]		1	2

[a] Not available in open literature, value predicted by GCA-EOS.

[b] Calculated from the normal boiling point of the pure compound.
[c] Calculated using the correlation of Espinosa et al. [54]

Acknowledgments

The authors acknowledge the financial support granted by the Consejo Nacional de Investigaciones Científicas y Técnicas (CONICET- PIP 11220110100454 / PIP 11220150100856 CO), the Ministerio de Ciencia, Tecnología e Innovación Productiva (MinCyT PICT 2012/1998 / PICT 2014/2293), and Universidad Nacional del Sur (UNS - 24/M133).

References

[1] J. Bonet, J. Costa, R. Sire, J.-M. Reneaume, A.E. Pleşu, V. Pleşu, G. Bozga, Revalorization of glycerol: Comestible oil from biodiesel synthesis, Food Bioprod. Process. 87 (2009) 171–178. doi:10.1016/j.fbp.2009.06.003.

[2] N. Rahmat, A.Z. Abdullah, A.R. Mohamed, Recent progress on innovative and potential technologies for glycerol transformation into fuel additives: A critical review, Renew. Sustain. Energy Rev. 14 (2010) 987–1000. doi:10.1016/j.rser.2009.11.010.

[3] P.D. Vaidya, A.E. Rodrigues, Glycerol Reforming for Hydrogen Production: A Review, Chem. Eng. Technol. 32 (2009) 1463–1469. doi:10.1002/ceat.200900120.

[4] L.J. Rovetto, M.E. Frontané, A.R. Vélez, L.E. Moyano, Thermodynamic study of hydrogen production from glycerol via supercritical water reforming PPEPPD 20013 – 13th International Conference on Properties and Phase Equilibria for Products and Process Design, in: 13th Int. Conf. Prop. Phase Equilibria Prod. Process Des., 2013: p. ID256.

[5] C.D. Kneupper, P.S. Basile, W.W. Fan, S. Noormann, Process and apparatus for producing and purifying epichlorohydrins, US8298500 B2, 2009. https://www.google.com/patents/WO2009108419A1?cl=en.

[6] M. Strebelle, P. Gilbeau, J.P. Catinat, Epichlorohydrin-based product and process for manufacturing this product, (2001). https://www.google.com/patents/US6288248.

[7] C. Len, R. Luque, Continuous flow transformations of glycerol to valuable products : an overview, Sustain. Chem. Process. 2 (2014) 1–10. doi:10.1186/2043-7129-2-1.

[8] M. Fiume, Final Report on the Safety Assessment of Triacetin, Int. J. Toxicol. 22 (2003) 1–10. doi:10.1177/1091581803022S203.

[9] S.H. Ogawa T, Moriwaki N, Fujii R, Tanaka K, Mori E, Saitou M, Yoshizawa H, Triacetin as food additive in gummy candy and other foodstuffs on the market., Kitasato Arch Exp Med. 65 (1992) 33–44. http://www.ncbi.nlm.nih.gov/pubmed/1479781.

[10] J.W. Lynch, J.W. Bailey, Dietary intake of the short-chain triglyceride triacetin vs. long-chain triglycerides decreases adipocyte diameter and fat deposition in rats, J. Nutr. 125 (1995) 1267–1273.

[11] H. Rastegari, H.S. Ghaziaskar, From glycerol as the by-product of biodiesel production to value-added monoacetin by continuous and selective esterification in acetic acid, J. Ind. Eng. Chem. 21 (2015) 856–861. doi:10.1016/j.jiec.2014.04.023.

[12] M. Rezayat, H.S. Ghaziaskar, Continuous extraction of glycerol acetates from their mixture using supercritical carbon dioxide, J. Supercrit. Fluids. 55 (2011) 937–943. doi:10.1016/j.supflu.2010.10.027.

[13] L.J. Florusse, A. van't Hof, T. Fornari, S.B. Bottini, C.J. Peters, Phase behavior of binary systems of carbon dioxide and certain low-molecular weight triglycerides: measurements and thermodynamic modeling, in: G.-H. Brunner, I. Kikic, M. Perrut (Eds.), 6th Int. Symp. Supercrit. Fluids, International Society for the Advancement of Supercritical Fluids, Versailles, France, 2003: p. PTs34. http://www.isasf.net/fileadmin/files/Docs/Versailles/Index.htm.

[14] P.E. Hegel, G.D.B. Mabe, M.S. Zabaloy, S. Pereda, E.A. Brignole, Liquid - Liquid - Supercritical Fluid Equilibria for Systems Containing Carbon Dioxide, Propane, and Triglycerides, J. Chem. Eng. Data. 54 (2009) 2085–2089. doi:10.1021/je800995r.

[15] P.H. van Konynenburg, R.L. Scott, Critical Lines and Phase Equilibria in Binary Van Der Waals Mixtures, Philos. Trans. R. Soc. A Math. Phys. Eng. Sci. 298 (1980) 495–540. doi:10.1098/rsta.1980.0266.

[16] A.V.M. Nunes, G.V.S.M. Carrera, V. Najdanovic-Visak, M. Nunes da Ponte, Solubility of CO2 in glycerol at high pressures, Fluid Phase Equilib. 358 (2013) 105–107. http://www.sciencedirect.com/science/article/pii/S0378381213004172 (accessed December 22, 2015).

[17] Y. Medina-Gonzalez, T. Tassaing, S. Camy, J.-S. Condoret, Phase equilibrium of the CO2/glycerol system: Experimental data by in situ FT-IR spectroscopy and thermodynamic modeling, J. Supercrit. Fluids. 73 (2013) 97–107. doi:10.1016/j.supflu.2012.11.012.

[18] H.P. Gros, S.B. Bottini, E.A. Brignole, A group contribution equation of state for associating mixtures, Fluid Phase Equilib. 116 (1996) 537–544. doi:10.1016/0378-3812(95)02928-1.

[19] S. Espinosa, M.S. Díaz, E.A. Brignole, Thermodynamic Modeling and Process Optimization of Supercritical Fluid Fractionation of Fish Oil Fatty Acid Ethyl Esters, Ind. Eng. Chem. Res. 41 (2002) 1516–1527. doi:10.1021/ie010470h.

[20] O. Ferreira, E.A. Macedo, E.A. Brignole, Application of the GCA-EoS model to the supercritical processing of fatty oil derivatives, J. Food Eng. 70 (2005) 579–587. doi:10.1016/j.jfoodeng.2004.10.012.

[21] P.E. Hegel, M.S. Zabaloy, G.D.B. Mabe, S. Pereda, E.A. Brignole, Phase equilibrium engineering of the extraction of oils from seeds using carbon dioxide+propane solvent mixtures, J. Supercrit. Fluids. 42 (2007) 318–324. doi:10.1016/j.supflu.2006.12.023.

[22] G. Soto, P.E. Hegel, S. Pereda, Supercritical production and fractionation of fatty acid esters and acylglycerols, J. Supercrit. Fluids. 93 (2014) 74–81. http://www.sciencedirect.com/science/article/pii/S0896844614001120 (accessed July 21, 2014).

[23] T. Fornari, C.F. Torres, G. Reglero, Simulation and Optimization of Supercritical Fluid Purilication 01 Phytosterol Esters, AIChE J. 55 (2009) 1023–1029. doi:10.1002/aic.

[24] F.A. Sánchez, T.M. Soria, S. Pereda, A.H. Mohammadi, D. Richon, E.A. Brignole, Phase Behavior Modeling of Alkyl - Amine + Water Mixtures and Prediction of Alkane Solubilities in Alkanolamine Aqueous Solutions with Group Contribution with Association Equation of State, Ind. Eng. Chem. Res. 49 (2010) 7085–7092. doi:10.1021/ie100421m.

[25] X. Liao, Y. Zhu, S.G. Wang, H. Chen, Y. Li, Theoretical elucidation of acetylating glycerol with acetic acid and acetic anhydride, Appl. Catal. B Environ. 94 (2010) 64–70. doi:10.1016/j.apcatb.2009.10.021.

[26] G.A. Bedogni, C.L. Padró, N.B. Okulik, A combined experimental and computational study of the esterification reaction of glycerol with acetic acid, J. Mol. Model. 20 (2014). doi:10.1007/s00894-014-2167-y.

[27] M. Cismondi Duarte, M.L. Michelsen, Global phase equilibrium calculations: Critical lines, critical end points and liquid–liquid–vapour equilibrium in binary mixtures, J. Supercrit. Fluids. 39 (2007) 287–295. http://www.sciencedirect.com/science/article/pii/S0896844606000908 (accessed November 29, 2013).

[28] M. Cismondi Duarte, M. Gaitán, Global Phase Equilibrium Calculations (GPEC), (2008). http://phasety.com/7/projects/gpec/.

[29] M.L. Michelsen, The isothermal flash problem. Part I. Stability, Fluid Phase Equilib. 9 (1982) 1–19. doi:10.1016/0378-3812(82)85001-2.

[30] M.L. Michelsen, The isothermal flash problem. Part II. Phase-split calculation, Fluid Phase Equilib. 9 (1982) 21–40. doi:10.1016/0378-3812(82)85002-4.

[31] E. Kehat, B. Ghitis, Simulation of an extraction column, Comput. Chem. Eng. 5 (1981) 171–180. doi:10.1016/0098-1354(81)85006-5.

[32] N.F. Carnahan, K.E. Starling, Equation of State for Nonattracting Rigid Spheres, J. Chem. Phys. 51 (1969) 635. doi:10.1063/1.1672048.

[33] G.A. Mansoori, N.F. Carnahan, K.E. Starling, T.W. Leland Jr., Equilibrium Thermodynamic Properties of the Mixture of Hard Spheres, J. Chem. Phys. 54 (1971) 1523–1525. doi:10.1063/1.1675048.

[34] D.S. Abrams, J.M. Prausnitz, Statistical thermodynamics of liquid mixtures: A new expression for the excess Gibbs energy of partly or completely miscible systems, AIChE J. 21 (1975) 116–128. doi:10.1002/aic.690210115.

[35] W.G. Chapman, K.E. Gubbins, G. Jackson, M. Radosz, SAFT: Equation-of-state solution model for associating fluids, Fluid Phase Equilib. 52 (1989) 31–38. doi:10.1016/0378-3812(89)80308-5.

[36] M. González Prieto, F.A. Sánchez, S. Pereda, Thermodynamic model for biomass processing in pressure intensified technologies, J. Supercrit. Fluids. 96 (2015) 53–67. doi:10.1016/j.supflu.2014.08.024.

[37] C.J. Gregg, F.P. Stein, M. Radosz, Phase Behavior of Telechelic Polyisobutylene in Subcritical and Supercritical Fluids. 4. SAFT Association Parameters from FTIR for Blank, Monohydroxy, and Dihydroxy PIB 200 in Ethane, Carbon Dioxide, and Chlorodifluoromethane, J. Phys. Chem. B. 103 (1999) 1167–1175. doi:10.1021/jp983157a.

[38] Design Institute for Physical Properties, BYU-DIPPR, Project 801 Evaluated Process Design Data, (1998).

[39] T.M. Soria, F.A. Sánchez, S. Pereda, S.B. Bottini, Modeling alcohol+water+hydrocarbon mixtures with the group contribution with association equation of state GCA-EoS, Fluid Phase Equilib. 296 (2010) 116–124. doi:10.1016/j.fluid.2010.02.040.

[40] D. Ambrose, D.J. Hall, Thermodynamic properties of organic oxygen compounds L. The vapour pressures of 1,2-ethanediol (ethylene glycol) and bis(2-hydroxyethyl) ether (diethylene glycol), J. Chem. Thermodyn. 13 (1981) 61–66. doi:10.1016/S0021-9614(81)80009-2.

[41] S.P. Verevkin, Determination of vapor pressures and enthalpies of vaporization of 1,2-alkanediols, Fluid Phase Equilib. 224 (2004) 23–29. doi:10.1016/j.fluid.2004.05.010.

[42] D.M. VonNiederhausern, L.C. Wilson, N.F. Giles, G.M. Wilson, Critical-Point Measurements for Nine Compounds by a Flow Method, J. Chem. Eng. Data. 45 (2000) 154–156. doi:10.1021/je990189y.

[43] W. V. Steele, R.D. Chirico, S.E. Knipmeyer, A. Nguyen, Measurements of Vapor Pressure,

Heat Capacity, and Density along the Saturation Line for ε-Caprolactam, Pyrazine, 1,2-Propanediol, Triethylene Glycol, Phenyl Acetylene, and Diphenyl Acetylene, J. Chem. Eng. Data. 47 (2002) 689–699. doi:10.1021/je010085z.

[44] W. V. Steele, R.D. Chirico, S.E. Knipmeyer, A. Nguyen, Vapor Pressure of Acetophenone, (±)-1,2-Butanediol, (±)-1,3-Butanediol, Diethylene Glycol Monopropyl Ether, 1,3-Dimethyladamantane, 2-Ethoxyethyl Acetate, Ethyl Octyl Sulfide, and Pentyl Acetate, J. Chem. Eng. Data. 41 (1996) 1255–1268. doi:10.1021/je9601117.

[45] Verevkin, S. P., Vapor Pressures and Enthalpies of Vaporization of a Series of the 1,3-Alkanediols, J. Chem. Eng. Data. 52 (2007) 301–308. doi:10.1021/je060419q.

[46] VonNiederhausern, D.M. Wilson, G.G. M., F. Neil, Critical Point and Vapor Pressure Measurements for 17 Compounds by a Low Residence Time Flow Method †, J. Chem. Eng. Data. 51 (2006) 1990–1995. doi:10.1021/je060269j.

[47] A.C. Galvão, A.Z. Francesconi, Experimental study of methane and carbon dioxide solubility in 1,4-butylene glycol at pressures up to 11MPa and temperatures ranging from 303 to 423K, J. Supercrit. Fluids. 51 (2009) 123–127. doi:10.1016/j.supflu.2009.08.012.

[48] M. González Prieto, F.A. Sánchez, S. Pereda, Multiphase Equilibria Modeling with GCA-EoS. Part I: Carbon Dioxide with the Homologous Series of Alkanes up to 36 Carbons, Ind. Eng. Chem. Res. 54 (2015) 12415–12427. doi:10.1021/acs.iecr.5b03269.

[49] M. González Prieto, F.A. Sánchez, S. Pereda, Fluid phase equilibria modeling of carbon dioxide with alkanes, alcohols and water with the GCA-EoS, in: 27th Eur. Symp. Appl. Thermodyn., Eidhoven, Holland, 2014: p. O5. doi:10.13140/2.1.3282.0002.

[50] A. Bamberger, G. Maurer, High-pressure (vapour + liquid) equilibria in (carbon dioxide+ acetone or 2-propanol) at temperatures from 293 K to 333 K, J. Chem. Thermodyn. 32 (2000) 685–700. doi:10.1006/jcht.1999.0641.

[51] R.M.M. Stevens, J.C. van Roermund, M.D. Jager, T.W. de Loos, J. de Swaan Arons, High-pressure vapour-liquid equilibria in the systems carbon dioxide + 2-butanol, + 2-butyl acetate, + vinyl acetate and calculations with three EOS methods, Fluid Phase Equilib. 138 (1997) 159–178. doi:10.1016/S0378-3812(97)00163-5.

[52] H. Inomata, A. Kondo, H. Kakehashi, Vapor–liquid equilibria for CO2–fermentation alcohol mixtures, Fluid Phase Equilib. 228–229 (2005) 335–343. doi:10.1016/j.fluid.2004.09.033.

[53] N.S. Cotabarren, P.E. Hegel, S. Pereda, Thermodynamic model for process design, simulation and optimization in the production of biodiesel, Fluid Phase Equilib. 362 (2014) 108–112. doi:10.1016/j.fluid.2013.09.019.

[54] S. Espinosa, T. Fornari, S.B. Bottini, E.A. Brignole, Phase equilibria in mixtures of fatty oils and derivatives with near critical fluids using the GC-EOS model, J. Supercrit. Fluids. 23 (2002) 91–102. doi:10.1016/S0896-8446(02)00025-6.

[55] A. Bondi, van der Waals Volumes and Radii, J. Phys. Chem. 68 (1964) 441–451. doi:10.1021/j100785a001.

[56] S.P. Verevkin, S.A. Kozlova, V.N. Emel'yanenko, E.D. Nikitin, A.P. Popov, E.L. Krasnykh, Vapor pressures, enthalpies of vaporization, and critical parameters of a series of linear aliphatic dimethyl esters of dicarboxylic acids, J. Chem. Eng. Data. 51 (2006) 1896–1905. doi:10.1021/je0602418.

[57] H. Katayama, Measurement and Estimation of Vapor Pressures of Dimethyl, Diethyl, Diisopropyl and Dibutyl Succinates at Reduced Pressure, J. Chem. Eng. Japan. 25 (1992) 366–372.

[58] D. Ambrose, C. Tsonopoulos, E.D. Nikitin, D.W. Morton, K.N. Marsh, Vapor–Liquid Critical

Properties of Elements and Compounds. 12. Review of Recent Data for Hydrocarbons and Non-hydrocarbons, J. Chem. Eng. Data. 60 (2015) 3444–3482. doi:10.1021/acs.jced.5b00571.

[59] B.C.Y. Lu, T. Ishikawa, G.C. Benson, Isothermal vapor-liquid equilibria for n-hexane-methyl methacrylate, methyl n-propyl ketone-acetic acid, n-pentane-methyl acetate, and ethyl acetate-acetic anhydride, J. Chem. Eng. Data. 35 (1990) 331–334. doi:10.1021/je00061a029.

[60] J. Acosta, A. Arce, J. Martínez-Ageitos, E. Rodil, A. Soto, Vapor−Liquid Equilibrium of the Ternary System Ethyl Acetate + Hexane + Acetone at 101.32 kPa, J. Chem. Eng. Data. 47 (2002) 849–854. doi:10.1021/je0102917.

[61] L.-C. Feng, C.-H. Chou, M. Tang, Y.-P. Chen, Vapor-Liquid Equilibria of Binary Mixtures 2-Butanol + Butyl Acetate, Hexane + Butyl Acetate, and Cyclohexane + 2-Butanol at 101.3 kPa, J. Chem. Eng. Data. 43 (1998) 658–661. doi:10.1021/je9800205.

[62] H.-S. Byun, M.-Y. Choi, J.-S. Lim, High-pressure phase behavior and modeling of binary mixtures for alkyl acetate in supercritical carbon dioxide, J. Supercrit. Fluids. 37 (2006) 323–332. doi:10.1016/j.supflu.2005.10.007.

[63] M. Kato, D. Kodama, M. Sato, K. Sugiyama, Volumetric Behavior and Saturated Pressure for Carbon Dioxide + Ethyl Acetate at a Temperature of 313.15 K, J. Chem. Eng. Data. 51 (2006) 1031–1034. doi:10.1021/je050514j.

[64] S. Sima, V. Feroiu, D. Geană, New high pressure vapor-liquid equilibrium data and density predictions for carbon dioxide+ethyl acetate system, Fluid Phase Equilib. 325 (2012) 45–52. doi:10.1016/j.fluid.2012.03.028.

[65] G.R. Borges, A. Junges, E. Franceschi, F.C. Corazza, M.L. Corazza, J.V. Oliveira, C. Dariva, High-Pressure Vapor−Liquid Equilibrium Data for Systems Involving Carbon Dioxide + Organic Solvent + β-Carotene, J. Chem. Eng. Data. 52 (2007) 1437–1441. doi:10.1021/je700125v.

[66] A. Chrisochoou, K. Schaber, U. Bolz, Phase equilibria for enzyme-catalyzed reactions in supercritical carbon dioxide, Fluid Phase Equilib. 108 (1995) 1–14. doi:10.1016/0378-3812(95)02696-C.

[67] D. Kodama, K. Sugiyama, T. Ono, M. Kato, Volumetric properties of carbon dioxide+isopropyl ethanoate mixtures at 308.15 and 313.15K, J. Supercrit. Fluids. 47 (2008) 128–134. http://www.sciencedirect.com/science/article/pii/S0896844608002404 (accessed March 25, 2016).

[68] J. Pavlíček, G. Bogdanić, I. Wichterle, Vapour–liquid and chemical equilibria in the ethyl ethanoate+ethanol+propyl ethanoate+propanol system accompanied with transesterification reaction, Fluid Phase Equilib. 328 (2012) 61–68. doi:10.1016/j.fluid.2012.05.016.

[69] P. Murti, M. Van Winkle, Vapor-Liquid Equilibria for Binary Systems of Methanol, Ethyl Alcohol, 1-Propanol, and 2-Propanol with Ethyl Acetate and 1-Propanol-Water., Ind. Eng. Chem. Chem. Eng. Data Ser. 3 (1958) 72–81. doi:10.1021/i460003a016.

[70] G.-B. Hong, M.-J. Lee, H. Lin, Multiphase Coexistence for Mixtures Containing Water, 2-Propanol, and Isopropyl Acetate, Ind. Eng. Chem. Res. 42 (2003) 937–944. doi:10.1021/ie020583g.

[71] B. Schmid, M. Döker, J. Gmehling, Measurement of the thermodynamic properties for the reactive system ethylene glycol–acetic acid, Fluid Phase Equilib. 258 (2007) 115–124. doi:10.1016/j.fluid.2007.05.030.

[72] S.P. Verevkin, V.N. Emel'yanenko, A. V. Toktonov, A.S. Leolko, J. Duwensee, U. Kragl, S.M.

Sarge, Thermochemical and Ab initio studies of biodiesel fuel surrogates: 1,2,3-propanetriol triacetate, 1,2-ethanediol diacetate, and 1,2-ethanediol monoacetate, Ind. Eng. Chem. Res. 48 (2009) 7388–7399. doi:10.1021/ie900308u.

[73] A.L. Woodman, A. Adicoff, Vapor Pressure of Triacetin, Triethylene Glycol Dinitrate, and Metriol Trinitrate, 8 (1963) 1–2.

[74] A.S. Maslakova, E.L. Krasnykh, S. V. Levanova, Saturated vapor pressures and enthalpies of evaporation of esters of glycerol and lower carboxylic acids, Russ. J. Phys. Chem. A. 84 (2010) 163–168. doi:10.1134/S0036024410020032.

[75] F.J. Baur, Crystalline Triacetin, J. Phys. Chem. 58 (1954) 380–380. doi:10.1021/j150514a021.

[76] T. Daubert, G. Hutchison, Vapor Pressure of 18 Pure IndustrialChemicals, in: Am. Inst. Chem. Eng. Symp., New York, 1990.

[77] R.E. Dunbar, L.L. Bolstad, Notes - The Acetylation of Organic Hydroxy Compounds with Ketene, J. Org. Chem. 21 (1956) 1041–1044. doi:10.1021/jo01115a613.

[78] S.F. Shakhova, T.I. Bondareva, Z. Y.P., Solubilities of Carbon Dioxide and Hydrogen Sulfide in Organics Solvents, Khim.Prom-St (Moscow). 10 (1966) 753–755.

[79] E.A. Brignole, S. Pereda, eds., Phase Equilibrium Engineering, 1st ed., Elsevier B.V., Amsterdam, The Netherlands, 2013. http://www.sciencedirect.com/science/bookseries/22120505/3/supp/C.

[80] S. Pereda, S. Raeissi, A.E. Andreatta, S.B. Bottini, M. Kroon, C.J. Peters, Modeling gas solubilities in imidazolium based ionic liquids with the [Tf2N] anion using the GC-EoS, Fluid Phase Equilib. 409 (2016) 408–416. doi:10.1016/j.fluid.2015.10.037.

[81] S. Skjold-Jørgensen, Group contribution equation of state (GC-EOS): a predictive method for phase equilibrium computations over wide ranges of temperature and pressures up to 30 MPa, Ind. Eng. Chem. Res. 27 (1988) 110–118.

[82] T.M. Soria, A.E. Andreatta, S. Pereda, S.B. Bottini, Thermodynamic modeling of phase equilibria in biorefineries, Fluid Phase Equilib. 302 (2011) 1–9. doi:10.1016/j.fluid.2010.10.029.

[83] M. Kato, K. Sugiyama, M. Sato, D. Kodama, Volumetric property for carbon dioxide+methyl acetate system at 313.15K, Fluid Phase Equilib. 257 (2007) 207–211. http://www.sciencedirect.com/science/article/pii/S037838120700057X (accessed March 14, 2016).

[84] L.J. Florusse, T. Fornari, S.B. Bottini, C.J. Peters, Phase behavior of carbon dioxide—low-molecular weight triglycerides binary systems: measurements and thermodynamic modeling, J. Supercrit. Fluids. 31 (2004) 123–132. doi:10.1016/j.supflu.2003.10.004.

[85] Y.-H. Fu, S.I. Sandler, A Simplified SAFT Equation of State for Associating Compounds and Mixtures, Ind. Eng. Chem. Res. 34 (1995) 1897–1909. doi:10.1021/ie00044a042.